AALBORG UNIVERSITY
STUDENT REPORT

Removal of Sour Gases Using Algae Derived Activated Carbon

Josefine Rønn Jakobsen

Master Thesis 2016

Oil and Gas Technology

Aalborg Universitet Esbjerg

Niels Bohrs vej 8, 6700 Esbjerg

Title Sheet

Theme:	Gas separation
Project title:	Removal of sour gases using algae derived activated carbon
Semester:	10th semester
Group number:	K10OG-6-F16
Supervisor:	Erik Gydesen Søgaard
University:	Aalborg University Esbjerg
Project period	1/2-2016 - 9/6-2016
Initial problem:	How is activated carbon synthesised from algae, which activation method gives the highest surface area, and how is the adsorption properties towards sour gases?

Josefine Rønn Jakobsen

Preface

This project is an 10th semester project which was written in the spring of 2016 by student Josefine Rønn Jakobsen, enrolled in the Oil and Gas Technology Masters program at Aalborg University Esbjerg.

The bibliography is found in the back of the report, on page 100. The references are enclosed in square brackets such as [X] and the sources are referred to using numbers which then can be found in the bibliography.

In this report a decimal number will be represented by a dot (.) while separation of thousands is represented by a comma (,).

After the prospects appendixes can be found.

A CD is attached to the report containing an electronic version of the report.

Acknowledgements

I would like to thank:

AlgeCenter Danmark for providing the microalgae Scenedesmus for my research.

Vittorio Boffa, associate professor at the Department of Chemistry and Bioscience at Aalborg University, for preparing my activated carbons samples.

The laboratory staff of Aalborg University Esbjerg for their great help with various equipment.

Abstract

The present report is a study of algae derived activated carbon which purpose was to adsorb hydrogen sulphide. In the oil and gas industry hydrogen sulphide is known to be a corrosive and toxic gas which even at low concentrations is lethal to humans. Together with carbon dioxide they make up the sour gases in an oil and gas reservoir. In this report the theory behind the adsorption process and the adsorption method is compared to the current methods for removal of sour gases. Also different materials used for adsorbents are briefly discussed however the main focus is on algae derived activated carbons. The whole process from raw algae material to activated carbon is described and tested. Several samples were prepared using different techniques. These samples were compared in different ways. The surface area were determined using the BET theory and the pore size distribution was determined using the Dollimore-Heal theory. The adsorption of hydrogen sulphide was tested using and simple adosrpiton setup and the samples were tested using elemental analysis. This way it was possible to figure out which sample was favourable for adsorption of hydrogen sulphide. This report presents a method to synthesis and analyse activated carbon derived from an organic compound. The main purpose was then to test the materials in order to see if they fulfil the demands for an activated carbon material.

Contents

Introduction

Natural gas is one of the fluids which can be found in a production well. It coexists with oil and water and together they make up the total amount of production fluids. Often non-hydrocarbon compounds exist in the gas phase, compounds which are highly unwanted. Two of them are carbon dioxide and hydrogen sulphide, together called sour gases due to their acidic nature. Specially for hydrogen sulphide certain limits apply for the content in natural gas. Because carbon dioxide and hydrogen sulphide are sour gases their corrosive nature is harmful to pipes and equipment. Furthermore hydrogen sulphide is highly hazardous to humans even at low concentrations.

Methods such as scavenging and absorption for removal of sour gases have already been tested. However no methods so far has proven itself as a very good solution. While scavengers can cause problems downstream, absorption systems require expensive absorption materials and equipment. Therefore this project will explore the potential of using adsorption for removal of sour gases. Adsorption materials can be produced from waste products such as corncob, rice husk and sawdust. However some cheap materials can also be produced only for the purpose of producing activated carbon. As example algae is a fairly cheap and simple material to produce under the right conditions. Algae have the advantage of having a high carbon content. Therefore, algae were used in this project for the synthesis of activated carbon. This led to the initiating problem of this project:

How is activated carbon synthesised from algae, which activation method gives the highest surface area, and how is the adsorption properties towards sour gases?

In order to answer these questions different activation techniques were tested and compared using a well known method for calculation of specific surface area of porous materials. However, the surface area would not be enough to determine the success of the activation. Also the adsorption properties of the material had to be tested. Even though the material might be porous it might not be able to perform physical adsorption of sour gases.

CHAPTER 1

Sour Gases in Natural Gas

An oil and gas well produces a stream of fluids which often is a mixture of liquid hydrocarbons (oil), gaseous hydrocarbons (natural gas), and water. In all three phases there are unwanted constituents whereof some must be removed. One of the most dangerous compounds found in all three phases is hydrogen sulphide (H_2S). In a previous study [1] it was proven with simulations that 60% of the total amount of H_2S is existing in the gas phase after separation. Therefore this phase is the most critical in case of H_2S. Together with carbon dioxide (CO_2) are called sour gases. Sour gases are unwanted due to their corrosive nature. It is expected the CO_2 distribution in the three phases is approximately the same as for H_2S. When a gas contains a considerable amount of CO_2 and H_2S it is considered to be sour.

1.1 Natural Gas

A typical composition of natural gas is shown in table 1.1. The only non-hydrocarbon gases in natural gas are; CO_2, H_2S, nitrogen (N_2), and helium (He). The amount of CO_2 and H_2S are almost equal, there is only a little more N_2 and the amount of helium in natural gas is almost zero. The total amount of gas produced at the Mærsk installation Gorm is 350,000 $\frac{m^3}{day}$ [2]. That means according to table 1.1 the gas stream would contain between 3500-7000 $\frac{m^3}{day}$ of CO_2, between 3500-7000 $\frac{m^3}{day}$ of H_2S, and between 3500-17500 $\frac{m^3}{day}$ of N_2.

Table 1.1: Composition of natural gas. [3]

Name	**Formula**	**% V/V**
Methane	CH_4	>85
Ethane	C_2H_6	3-8
Propane	C_3H_8	1-5
Butane	C_4H_{10}	1-2
Pentane*	C_5H_{12}*	1-5
Carbon dioxide	CO_2	1-2
Hydrogen Sulphide	H_2S	1-2
Nitrogen	N_2	1-5
Helium	He	<0.5
* Pentane and hydrocarbons of higher molecular weight including benzene and toluene.		

The sour gases in natural gas can be removed before and after separation from the other production fluids. For simplicity only removal of sour gases in the gas phase is investigated in this project. Figure 1.1 shows the overall separation processes of the production fluids. The separation of the sour gases from natural gas could be performed at point (3) where the gas treatment is performed. Due to the corrosive nature of the sour gases equipment, pipes etc. might be damaged and in 2008 it was estimated by the National Association of Corrosion Engineers that the expenses due to corrosion in the oil and gas industry reached almost 1.4 billion US dollars [4]. Therefore the efficiency of the removal of corrosive constituents is essential.

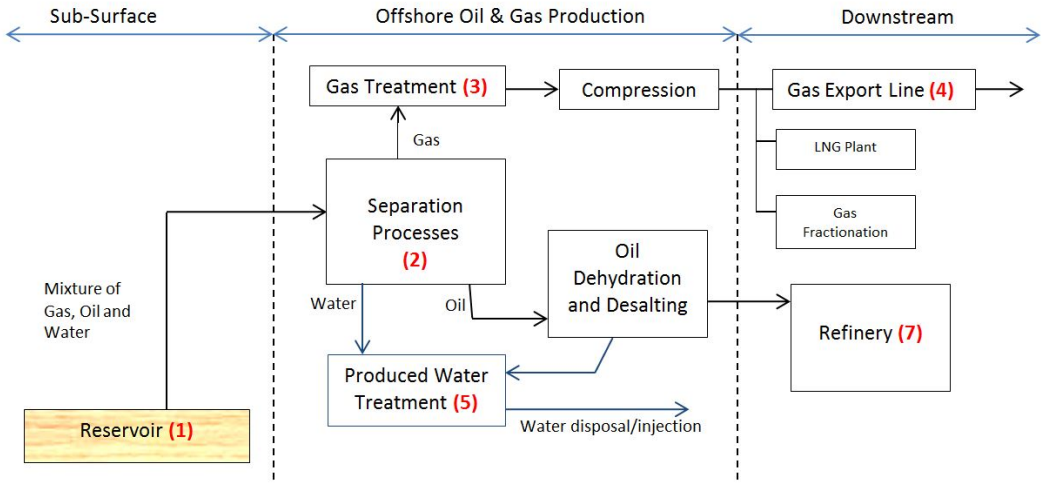

Figure 1.1: Block diagram of the main separation processes of production fluids. [1]

The most important factors to consider when evaluating possible ways to remove sour gases are [5];

- performance,
- price,
- stability,
- health and safety in handling and storage,
- environmental restrictions, and
- compatibility.

Often sour gases are removed using a scavenger which a chemical used to chemically convert the gases into less harmful compounds. However scavengers has been suspected for causing problems further downstream [6]. Since the use of chemicals can be costly too, other methods for removal of sour gases should be investigated.

1.2 Carbon Dioxide

Carbon dioxide (CO_2) is a corrosive, colourless gas. It makes up approximately 0.04 % of the total amount of components in the atmosphere. It is formed by different processes on Earth including respiration of animals and combustion of carbon materials. However it can also be consumed again by the photosynthesis of plants. In water CO_2 forms carbonic acid, a weak volatile acid. The solubility in water is 1.45 $\frac{g}{L}$ at room temperature and atmospheric pressure, and can therefore be found in rivers, lakes, ground water etc.. It is not harmful to humans. However as the amount of CO_2 in the atmosphere is increasing the amount in oceans and fresh waters are increasing too. This increases the pH of the water making it sour. This can cause problems for the plant and animal life living in the water.
There are different utilisations options for captured CO_2. First it can be used to cultivate algae for various purposes. Second it can be used for oil and gas processes such as enhanced oil recovery.

1.3 Hydrogen Sulphide

Hydrogen sulphide (H_2S) is a highly corrosive and toxic gas which can be found on oil and gas work sites. It is colourless, flammable and has a very distinctive smell of rotten eggs. As showed in a previous study [1] it exists in all three

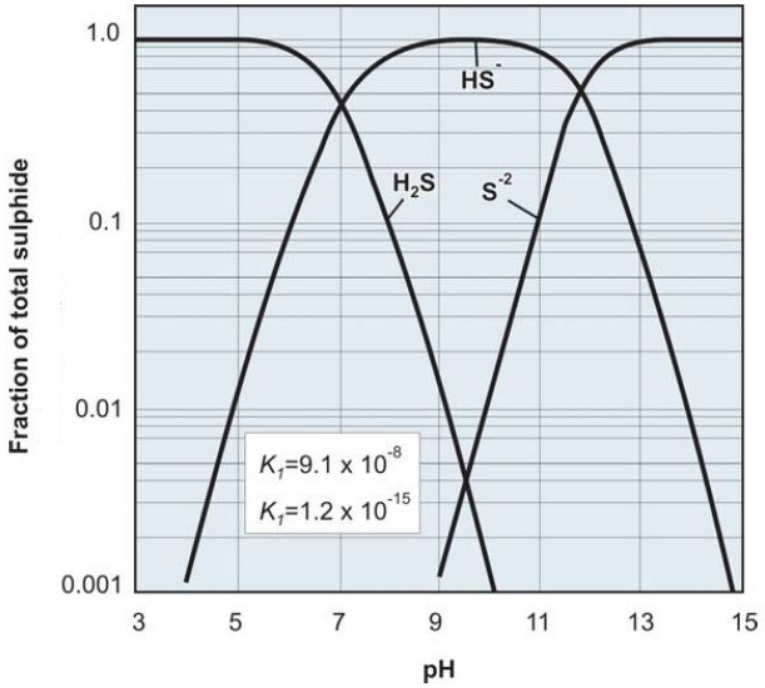

Figure 1.2: Ionisation chart for the distribution of sulphide for changing pH. [7]

phases. Its solubility in water is 3.3 $\frac{g}{L}$ at room temperature and atmospheric pressure. H_2S exist naturally in many wells due to different factors. One process producing H_2S is the decomposition of hydrocarbon with a high sulphur content. Another way for the H_2S to be produced is by sulphate reducing bacteria (SRB). SRB decompose sulphate ions reducing sulphate to sulphide. The decrease of redox potential leads to the release of H_2S. SRB are only active at temperatures below 140 $°C$ [5]. At temperatures above 140 $°C$ thermochemical sulphate reduction (TSR) occur [5]. TSR is a reaction where sulphate minerals are reduced by a reaction with hydrocarbons [5].
In water H_2S forms highly corrosive sulphuric acid. But also in pure form H_2S is unwanted. It is extremely toxic, even at low concentrations. It is required by most purchasers to have a concentration below 3-5 *ppm*.
H_2S can be neutralised by having a constant high pH as showed in figure 1.2. The figure shows how pH affects the sulphide. It is clear that having a pH above 11 will keep the sulphate in a less harmful form than H_2S. Table 1.2 shows the symptoms from H_2S exposure of different concentrations. It is clear that even at low concentrations H_2S can be very harmful.

Table 1.2: Symptoms and effects from exposure to different concentrations of H_2S [8].

Concentration (ppm)	**Symptoms/Effects**
0.00011-0.000033	Typical background concentrations.
0.01-1.5	Odor threshold (when rotten egg smell is first noticeable to some). Odor becomes more offensive at 3-5 ppm. Above 30 ppm, odor described as sweet or sickeningly sweet.
2-5	Prolonged exposure may cause nausea, tearing of the eyes, headaches or loss of sleep. Airway problems (bronchial constriction) in some asthma patients.
20	Possible fatigue, loss of appetite, headache, irritability, poor memory, dizziness.
50-100	Slight conjunctivitis ("gas eye") and respiratory tract irritation after 1 hour. May cause digestive upset and loss of appetite.
100	Coughing, eye irritation, loss of smell after 2-15 minutes (olfactory fatigue). Altered breathing, drowsiness after 15-30 minutes. Throat irritation after 1 hour. Gradual increase in severity of symptoms over several hours. Death may occur after 48 hours.
100-150	Loss of smell (olfactory fatigue or paralysis).
200-300	Marked conjunctivitis and respiratory tract irritation after 1 hour. Pulmonary edema may occur from prolonged exposure.
500-700	Staggering, collapse in 5 minutes. Serious damage to the eyes in 30 minutes. Death after 30-60 minutes.
700-1000	Rapid unconsciousness, "knockdown" or immediate collapse within 1 to 2 breaths, breathing stops, death within minutes.
1000	Nearly instant death.

1.4 Removal of Sour Gases

Due to the corrosive nature of the sour gases, most of them are removed to secure equipment from rupture. The most common method to remove sour gases is from the use of scavengers. Scavengers are chemicals which often are injected directly into the process stream which is also their great advantage. Often there is no space for equipment for removal of sour gases on an offshore installation, therefore scavenging has been the preferred process.

The chemical reacts with the sour gas and converts it to a less harmful compound. The most popular type of scavenger is triazine of which the most common is 1,3,5-tri-(2-hydroxyethyl)-hexahydro-s-triazine (HHTT). The reaction between HHTT and H_2S gives the two products; monoethanolamine (MEA) and 5-(2-hydrozyethyl)-1,3,5-dithiazine (dithiazine). MEA can also react as a scavenger and is therefore a very useful product of the reaction. Dithiazine on the other hand has been suspected to cause trouble further downstream [6]. It seems like that the reaction products of the scavenging process cause fouling issues at the refineries. Also unused scavenger can be problematic since the triazine HHTT also works as a biocide. A biocide has the ability to kill some types of bacteria. When the scavenger and reactions products are separated from the natural gas it contains a certain amount of water. This water has to be treated. Often water treatment plants use bacteria to clean the water, but if some of the water to be cleaned contained a significant amount of unused HHTT the bacteria could be killed.

Other options for removal of sour gases are absorption units and membranes. Absorption units can be expensive and demands a lot of space. In the process the gas containing the sour gases is injected into the bottom of an adsorption column as shown in figure 1.3. Meanwhile a liquid is injected at the top. When the two phases meet the liquid phase can adsorb the sour gases. To do this the liquid must be selective towards acidic gases. A choice could be an amine solution.

For membrane permeation a polymeric membrane is used to filtrate the sour gases from the natural gas. The method is shown in figure 1.4. The membrane works as a result of a concentration gradient where gases dissolve through the membrane. This is also called membrane permeation. The membrane can either be designed to let natural gas through and leave CO_2 behind or the opposite. However it should be considered that membranes might not be 100% effective and complete separation might not be possible. Therefore alternatives for scavengers should be explored. The best solution would be to remove the unwanted compounds without adding anything to the natural gas since that

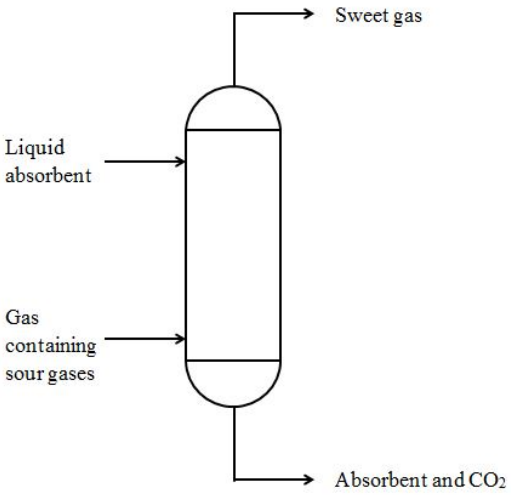

Figure 1.3: Illustration of an absorption column. The liquid adsorbent enters at the top while the gas containing CO_2 enters at the bottom. When the two phases contact CO_2 is absorbed by the liquid and leaves the column in the liquid phase. [9]

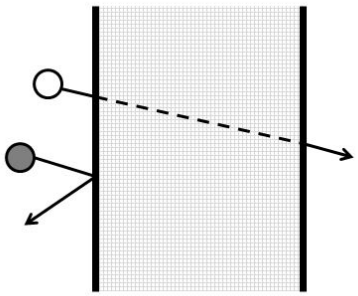

Figure 1.4: Illustration of membrane permeation. The white molecule can diffuse through the membrane while the grey cannot. [9]

might cause unexpected problems later in the process. That is why adsorption might be a good alternative. Often adsorption is performed in a column. The column contains granular or powdered activated carbon as shown in figure 1.5. In theory, by forcing the gas through the filter, containing several steps for removing sour gases, clean gas will exit the filter leaving the sour gases adsorbed onto activated carbon inside the filter. This can be done until the breakthrough of the sour gases are higher than the limit. Then it is time to either change the filter unit or clean it. Either way one thing is common, no material will be added to the process stream, only removal of compounds will occur. The unknown is which compounds are removed by the filter and thereby which compounds are the filter more selective towards?

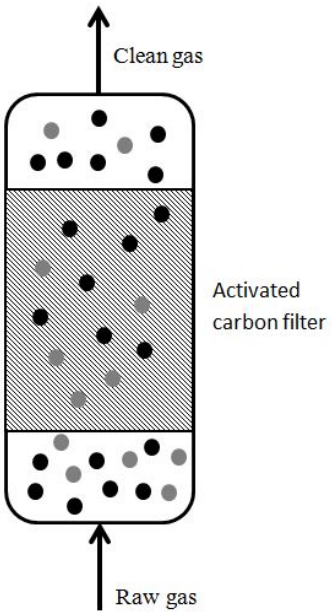

Figure 1.5: Adsorption unit containing powdered or granular activated carbon fixed in a filter. [9]

It is very important that the activated carbon in the filter is selective towards sour gases, if not it is possible that as an example CH_4 is adsorbed onto the activated carbon. Since CH_4 is the main product in natural gas it is highly unwanted to have it adsorbed onto activated carbon. An idea to overcome that the problem is to perform a washing step of the gas before adsorption. Offshore seawater is available in unlimited quantities and can therefore be used for washing the natural gas. CO_2 and H_2S has, as reported in section 1.2 and section 1.3, a high solubility in water. Therefore the idea is to dissolve CO_2 and H_2S in the water since CH_2 and N_2 have a solubility less than 0.02 $\frac{g}{L}$ at room temperature and atmospheric pressure. Hereafter the solution can be filtrated in a activated carbon filter removing the sour gases from the water. This could for example be done onshore.

Table 1.3 shows a comparison of the different methods. All have their advantages and disadvantages. For this project it was chosen to look deeper into the usage of activated carbons for removal of sour gases. The reason for this is the possibility to use cheap material for the synthesis.

Table 1.3: Comparison of the different separation methods. [9]

	Advantages	**Disadvantages**
Chemical conversion	Can be done in line meaning no need for extra equipment.	Difficult or impossible to retrieve the CO_2.
Absorption and stripping	Depending on the absorption type it can be reversible. It is easier to create contact compared to chemical conversion.	Costly process which demands a lot of equipment. Highly dependent of partial pressure for physical absorption. Loss of absorbent in the process.
Adsorption	Depending on the adsorption type it can be reversible. Adsorbents can be produced from a variety of waste materials. They can be tailored to have a higher selectivity towards certain compounds.	Costly process which demands a lot of equipment. Highly depends on the quality of the adsorbent. Adsorbents are costly to produce.
Membrane permeation	Possible to produce membranes for specific purposes. No moving parts reducing the maintenance.	Membranes can be expensive to produce. Fouling cause the efficiency to drop relatively fast.

CHAPTER 2

Algae

Algae is an organism able that utilises photosynthesis to produce oxygen and sugar from sunlight and CO_2. The unique thing about algae is that it comes in many different sizes. The smallest type of algae is plankton which has a size range of 0.5 μm to 1 mm. The largest type of algae can be up to 60 m. But algae can also be distinguished in other ways than size. For example their colour tels a lot about their structure. Green algae can have up to seven different layers in their cell wall while brown algae can only have one. The cell walls are composed of [10]:

- Cellulose, which is the main component.
- Alginat which is found in brown algae build from linear polymers.
- Agar is found in red algae as long chained agarbiose.
- Carrageenan which is different carbon hydrate polymers containing sulphate groups.
- Mannaner which is C6 carbon hydrates in green algae bound together with glucose.

One of the main advantages of algae is that it can be harvested continuously throughout the year unlike seasonal products such as different agricultural products. Also, algae can be grown in a large variety of water types such as wastewater, fresh water and brackish water. Unlike other plants algae does not have roots, leaves, and flowers [11]. Since algae grows much faster than land plants which, together with its ability to grow under different conditions, makes it a interesting plant for many different purposes such as synthesis of activated carbon.

2.1 Fucus Vesiculosus

Fucus vesiculosus, also known as bladderwrack, is a brown marine algae (seaweed) growing in the north western part of the world, including Danish shores. For this project the algae was collected at Elvig Høj Strand close to the city of Kolding at the Danish east coast. It grows on rocks and mussels in shallow water. It needs peaceful water to grow. It has bladders to keeps it floating but Fucus vesiculosus can also be found without bladders. Figure 2.1 shows how Fucus vesiculosus looks like. A very small amount of macroalgae was also

Figure 2.1: Danish Fucus vesiculosus. [12]

collected from the beach close to Esbjerg. This algae specie was unknown but it looked very much like Fucus Vesiculosus.

2.1.1 Comparison of Algae From Kolding and Esbjerg

The two algaes collected at a beach close to Kolding and Esbjerg were compared using elemental analysis. The method is described in appendix C. The results of the analysis are shown in table 2.1. It is shown that the content of carbon was highest in the algae from Kolding while the content of sulphur was highest in the algae from Esbjerg. The nitrogen content of the algae from Kolding is little bit higher than the algae from Esbjerg. If the nitrogen in the algae is bound in an amine group the properties of the algae could be alkaline and thereby the adsorption of sour gases would be higher.

Table 2.1: Elemental composition of macro algae from Kolding and Esbjerg.

Origin of algae	**Weight**	**Percentage**			
	$[mg]$	**Carbon**	**Hydrogen**	**Nitrogen**	**Sulphur**
Kolding	6.06	40.4	4.44	2.66	1.85
	4.488	40.08	5.33	2.44	1.99
	4.91	37.25	5	2.35	1.79
Esbjerg	3.707	35.86	5.14	2.1	2.5
	4.711	36.75	5.11	2.21	2.53
	5.143	36.79	5.16	2.2	2.37

2.2 Scenedesmus

Besides Fucus Vesiculosus the genus Scenedesmus was also used in this project. The algae was provided by AlgeCenter Danmark in Grenå. Scenedesmus is a green fresh water algae. It is a microalgae with either unicellular or simple multicellular structure [13]. Since it is a fresh water algae it is often found attached to rocks or wood but it can also exist as scum on stagnat water [14]. Scenedesmus belongs to a group of green algae called Chlorophyceae. Often Scenedesmus exists in colonies of 2, 4, or 8 cells arranged in a row [15]. The cells are mostly oval shaped [15]. A microscope photo of Scenedesmus obliquus and Scenedesmus opoliensis are showed in figures 2.2 and 2.3. Sometimes it can exist as a almost pure culture in fresh water plankton [16]. By having a low amount of phosphorous or low salt concentration the Scenedesmus will often grow unicellular [16]. The reason for their bright green colour is the high content of chlorophyll. The great advantage of using algae is the low cost for

Figure 2.2: Microscope photo of Scenedesmus obliquus. [15]

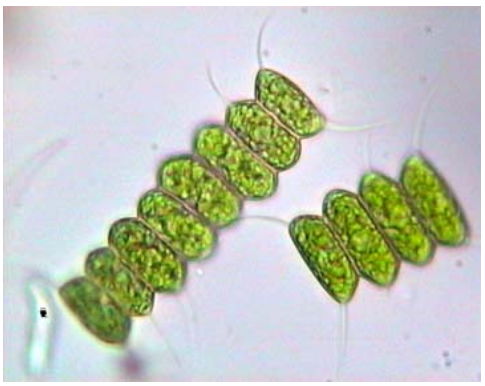

Figure 2.3: Microscope photo of Scenedesmus opoliensis.. [15]

production. Is does not require rich farm land and thereby not taking space from agricultural products used for food. Also it only needs water, nutrients, CO_2 and sunlight to grow making the growth of algae a low cost process.

2.3 Algae for Activated Carbon

In order to decide the success of the activation of algae derived carbon materials, it must be compared to similar studies. Table 2.2 shows the best results of different studies. The algae specie used as well as the activation method and highest achieved BET surface area are given. These studies can be compared with this study in order to determine the success. The first six studies were performed using macroalgae. The last study was performed using and unknown microalgae. The highest surface area was achieved by Lorenzo et al. [17] using the red macroalgae Gelidium. From these studies it seems like KOH chemical activation is the best solution since it gives the highest surface area for to different algae species.

Table 2.2: Comparison of algae derived activated carbons from different studies.

Author	**Algae specie**	**Activation method**	**Highest BET surface area** $[\frac{m^2}{g}]$
Aravindhan et al. [18]	Sargassum longifolium	Zinc chloride chemical activation	802
Aravindhan et al. [18]	Hypnea valentiae	Zinc chloride chemical activation	783
Pintor et al. [19]	Turbinaria turbinata	Pyrolysis	812
Lorenzo et al. [17]	Gelidium	KOH chemical activation	2118
Lorenzo et al. [17]	Gelidium	Microvawe activation	1100
Rathinam et al. [20]	Sargassum longifolium	Zinc chloride chemical activation	792
Jakobsen [9]	Uknown microalgae	KOH chemical activation	1539

CHAPTER 3

Activated Carbon

Porous materials can be used to separate compounds in a mixture of fluids. A cheap porous material which is also easy to produce is activated carbon. It can be synthesised from a large variety of raw materials such as corncob, rice husk, saw dust and algae. Activated carbon has been used successfully for water treatment for many years. However, activated carbon can besides separation of components from water also be used for separation of gases. The different properties of the activated carbon decides the application options. This chapter explores the basic theory of activated carbon.

3.1 Main Characteristics

Activated carbon is the definition of a porous carbon material which is usable for adsorption. The material can contain three different pore sizes;

- micropores: $<2\ nm$,
- mesopores: 2-50 nm, and
- macropores: $>50\ nm$.

In order to produce activated carbon a raw material must be chosen. The choice of raw material is very important as the chemistry of the material will together with the activation process decide the chemistry of the activated carbon. Many commercial activated carbon materials have a surface area around 1500 $\frac{m^2}{g}$. This means that if the material has a surface area considerably lower than that it is not regarded as activated carbon.

3.2 Activation

Activation can be performed in two different ways; through chemical activation or through physical activation. Both have their advantages and disadvantages and the method should be chosen having the choice of raw material in mind. The success of the activation is decided form the following factors;

- activation temperature,
- activation time,
- gas flow rate,
- choice of raw material,
- activating agent (if chemical activation is used),
- washing step (if chemical activation is used), and
- type of contact and ratio between raw material and activating agent (if chemical activation is used).

3.2.1 Physical Activation

Activation without the use of an activating agent is called physical activation. Instead a higher temperature must be used together with the pre-step called carbonisation. Physical activation is a thermal process where an oxidating gas or vapour such as CO_2 or steam (H_2O) is injected into a furnace containing the sample. The temperatures must be kept at 800 $°C$ or above in order for the following reactions to occur:

$$\begin{aligned} C + CO_2 &\rightleftharpoons 2CO \\ C + H_2O &\rightleftharpoons CO + H_2 \end{aligned} \tag{3.1}$$

The process removes less ordered carbon atoms in order to make pores. The products of the reactions, carbon monoxide (CO) and hydrogen gas (H_2), are removed by the flowing gas.
As mentioned, physical activation needs an extra pre-step in order to work optimally. This step is called carbonisation.

Carbonisation

Carbonisation is a pyrolysis process of the raw material. Organic matter is thermally degraded in the absence of oxygen in order to produce char. The temperature of the carbonisation process is often between 400-1000 $°C$.

There are three ways the material can be heated:

- Internally heating through combustion giving a high loss of material.
- External heating using another fuel.
- Hot circulating gas as heating source.

Hot circulating gas is often used as it gives possibility of oxygen exclusion resulting in a higher char quality.

3.2.2 Chemical Activation

Activation using an activating agent is called chemical activation. Often potassium hydroxide (KOH) is used as activating agent. Also for chemical activation heat must be applied. The expected reaction for chemical activation is [21]:

$$6KOH + 2C \rightleftharpoons 2K + 3H_2 + 2K_2CO_3 \tag{3.2}$$

Hydrogen gas (H_2) is removed by the flowing gas in the system. Potassium (K) and potasium carbonat (K_2CO_3) are expected to be found in solid form. The activation temperature for chemical activation is often between 600-1000 $°C$. For chemical activation it is not always necessary to perform carbonisation of the raw material if the material is completely dried and has a natural high carbon content. However, for chemical activation an extra washing step is performed after activation. This is done in order to remove K, K_2CO_3 as well as unreacted KOH, as they are highly water soluble. Because chemical activation includes the usage of an activating agent, one extra variable can be introduce as the ratio between the activating agent and the raw material.

Studies by as an example Ahmadpour et al. and Drage et al. [22, 23] indicated that chemical activation was better for creating a porous material with a certain pore structure. Therefore chemical activation was used for this project.

3.3 Adsorption

The process of which a fluid attaches to a solid surface is called adsorption. The fluid adsorbing on the surface is called the adsorbate and the solid surface is called the adsorbent.

There are two types of adsorption; physical and chemical adsorption.

Chemical adsorption is the process where the adsorbate attaches to the adsorbent due to transfer of electron resulting in a chemical bond. A chemical bond can require a large amount of energy to break making chemical adsorption not ideal when regeneration of the adsorption material is wanted.

Physical adsorption is based on the attraction between the adsorbate and the adsorbent. The attraction occurs due to van der Waals forces which requires dipole interactions between the adsorbent and the adsorbate. The process is always exothermic. For this project it was desired to adsorb CO_2 and H_2S on activated carbon. The chemical structure of CO_2 and H_2S are shown in figure 3.1 and 3.2. CO_2 has due to its linear structure a negative charge at each oxygen atom and therefore it needs a positive charged surface to attach to. H_2S has a v-shape where sulphur is much more electronegative than hydrogen meaning that there will be a negative charge around the sulphur molecule. Meanwhile there will be a positive charge at the two hydrogen atoms. Therefore H_2S can attach to both a positive and negative charged surface.

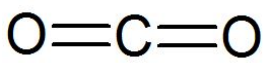

Figure 3.1: Molecular structure of CO_2.

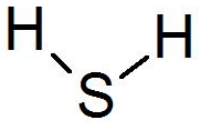

Figure 3.2: Molecular structure of H_2S.

3.3.1 The Adsorption Mechanism

The adsorption process can be divided into three phases;

- external mass transfer,
- internal mass transfer, and
- adsorption.

The three processes are shown in figure 3.3. The initial phase is the external mass transfer of the adsorbate. This part is defined as the mass transfer of adsorbate from the bulk to the external surface of the adsorbent. As the

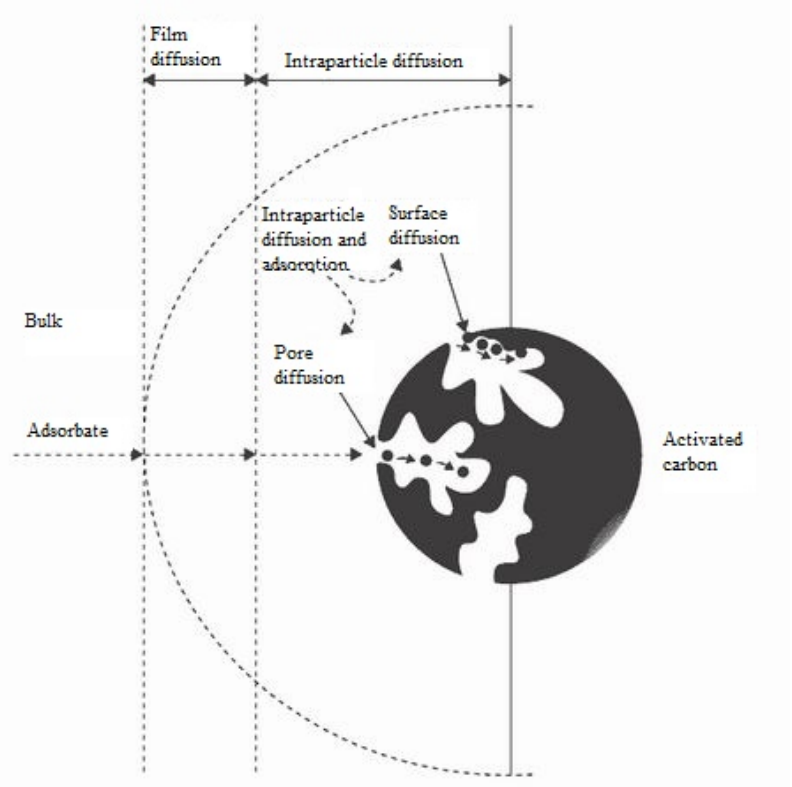

Figure 3.3: Illustration of the three phases of the adsorption process. [24]

adsorbate has reached the outer surface of the adsorbent the internal mass transfer can take place. This is the mass transfer of adsorbate inside the pores of the adsorbent. The internal mass transfer stops when the adsorbate reaches a site on which it can adsorb. Of the three processes the adsorption process is expected to be the fastest. Therefore in order to determine the rate of the process focus must be put on the transfer processes.

Certain factors can have an effect on the adsorption process. These are;

- surface area of adsorbent,
- physical and chemical characteristics of the adsorbate,
- pH,
- temperature,
- porosity of adsorbent, and
- chemical surface characteristics of adsorbent.

Often adsorption is given as a function of relative pressure of the adsorbate in a plot called adsorption isotherm. An example of an adsorption isotherm

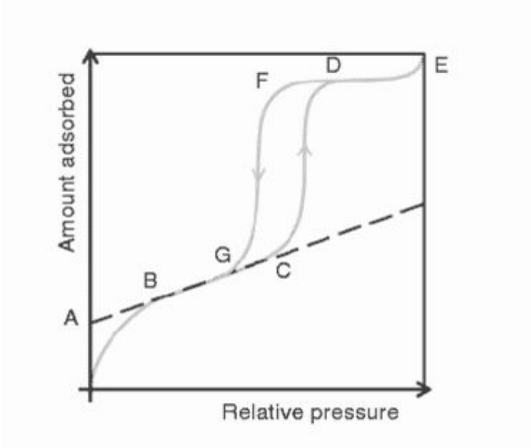

Figure 3.4: Illustration of an adsorption-desorption isotherm. The description of the figure is found in the text. [25]

is showed in figure 3.4. Point A gives the micropores filling also shown in figure 3.5. Point B in figure 3.4 is associated with the formation of a monolayer of gas on the surface. In the region between point B and C is the formation of the multilayer. In the region between point C and D are mesopore filled due to capillary condensation also shown in figure 3.6. The region between point D and E gives the end of the pore filling. Therefore the adsorbed amount at this point must represent the total pore volume. Point E to F is the beginning of the desorption branch. Point G shows where the desorption isotherm rejoins the adsorption isotherm. The space between the adsorption isotherm and the desorption isotherm can be used to define the porosity of the material.

As previously mentioned adsorption isotherms are used to determine the

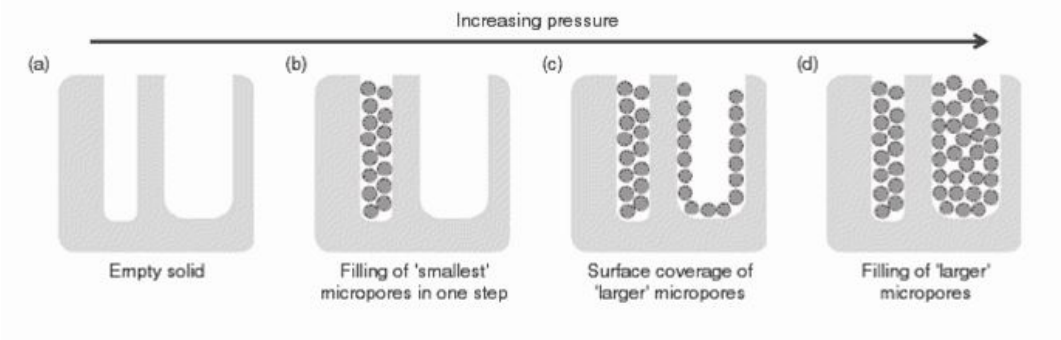

Figure 3.5: Illustration of the filling of micropores. Scenario (a) shows that a very low pressures the pores are empty. As the pressure is increased as in scenario (b), the smallest pores starts to fill. While increasing the pressure further the scenario in scenario (c) occurs. Here a layer will start to form on the surface of the larger micropores. If the pressure is increased further scenario (d) occur where all pores are filled. [25]

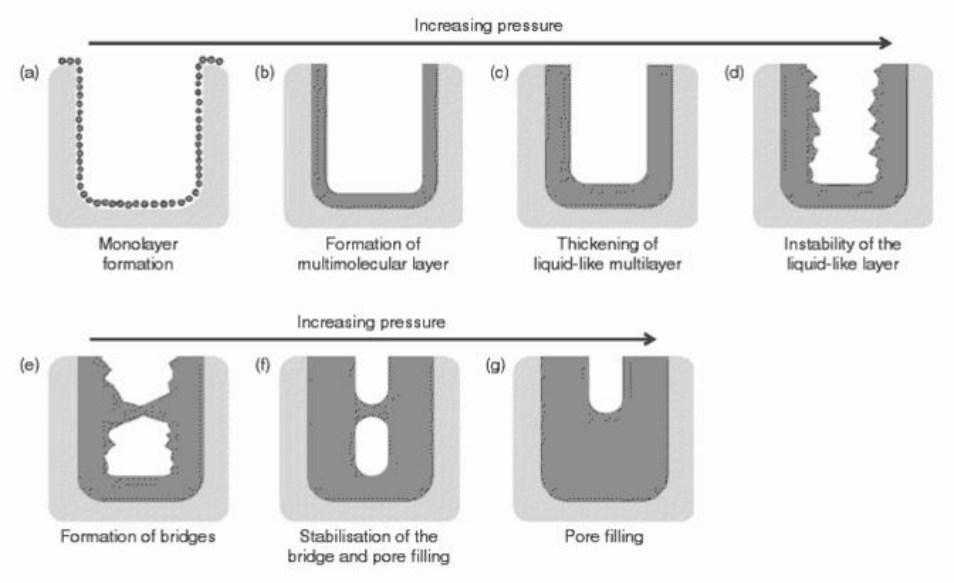

Figure 3.6: Illustration of the filling a mesopores. At low pressures a layer starts to develop at the surface as shown in scenario (a). By increasing the pressure gives scenario (b) where the layer becomes a multilayer. The layer hereafter thickens as shown in scenario (c). When the layer reach a certain thickens it will get unstable as shown in scenario (d). The instability may result in the formation of a bridge as shown in scenario (e). As the bridge stabilises the pore starts to fill again as given in scenario (f). Finally when the pressure is high the pore fills up as shown in scenario (g). [25]

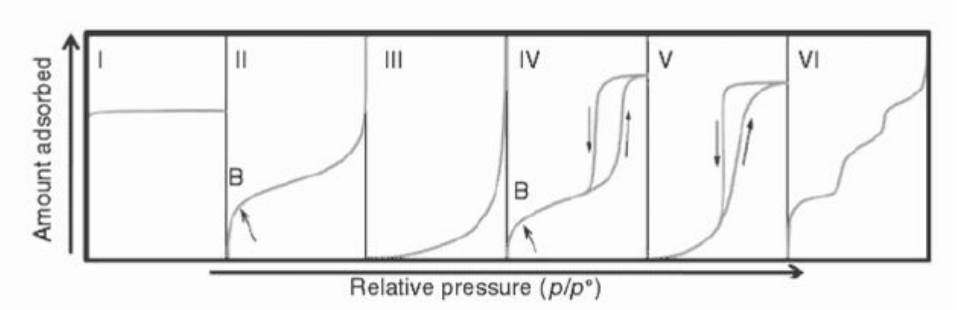

Figure 3.7: Illustration of the six isotherm types. [25]

success of the adsorption. The shape of the curve together with the area of the hysteresis loop determines the porosity. Figure 3.7 shows the six different isotherms. Type I represents microporosity as the pores fill at low pressure. Type II indicates that the material is non-porous. Type III indicates a non-porous and non-wetting adsorption. Type IV indicates that adsorption on a mesoporous solid occurs. Type V indicates adsoprtion on a mesoporous and non-wetting solid, which is an uncommon scenario. However, it is not only the isotherm type which can be used to describe the morphology of the material.

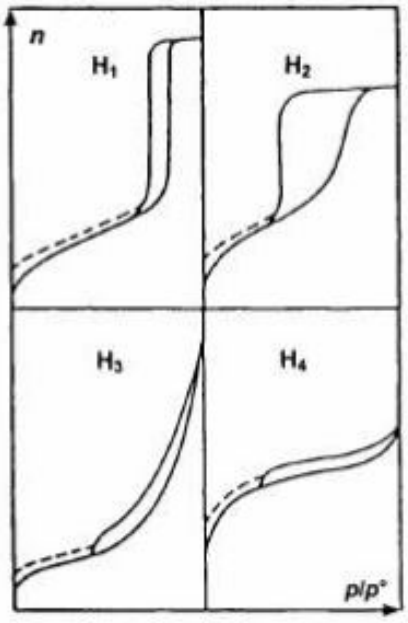

Figure 3.8: Illustration of the types of hysteresis loop. [26]

Also the shape and size of the hysteresis loop can be used to understand the pore structure. Figure 3.8 shows the different types of hysteresis loops of a adsorption-desorption isotherm. Starting with the type H1 loops, this type indicates that the adsorbent has a narrow uniform pore distribution [26]. For the type H2 loops it indicates that the pore structure is rather complex and is composed of interconnected networks of pores of different shapes and sizes [26]. Loops of type H3 indicates that the adsorbent has slit-shaped pores [26]. And finally loops of type H4 indicates a microporous adsorbent with slit-shapes pores [26].

3.4 Materials for Activated Carbon

Many different materials can be used for activated carbon. The main objective when choosing a raw material is to choose one with a naturally high carbon content. This will eliminate the need for extreme carbonisation of the material. Figure 3.9 shows an comparison of activated carbons prepared from

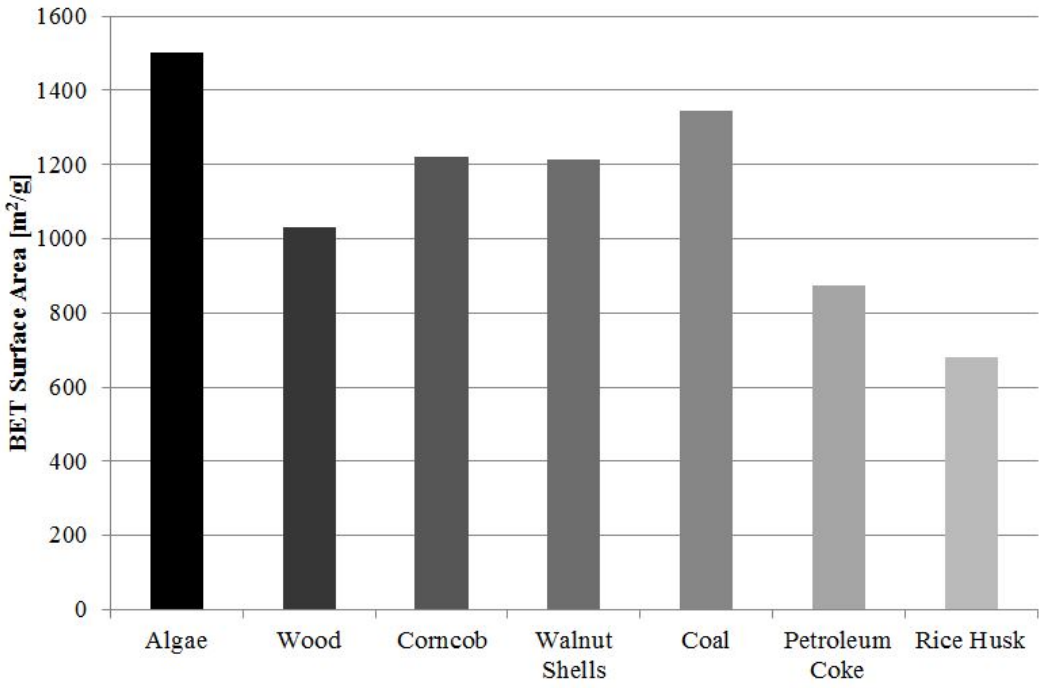

Figure 3.9: Comparison of activated carbon from different raw materials from different studies. All are prepared using the same method. [9]

different raw materials using the same method. From that study algae seemed to be a competitive choice for a raw material for activated carbon synthesis. However comparing with the surface areas in figure 2.2 it might not be the hole story. Most studies give a surface area of algae derived porous carbon of approximately 800 $\frac{m^2}{g}$ which is a bit lower than the average in the comparison in figure 3.9. Therefore this study might help to give an indication if the results from the studies by Lorenzo et al. [17] and Jakobsen [9] are unrealistic.

CHAPTER 4

Problem Evaluation

In the previous chapters the properties and issues concerning removal of sour gases from natural gas were addressed. The possibility for using activated carbon for removal was presented together with an idea for a raw material for the production of activated carbon. However there are some concerns to using algae derived activated carbon. Some of those concerns are:

- Does algae derived activated carbons have a sufficient surface area in order to be a good material for adsorption?
- How is the adsorption potential of sour gases?
- Which methods are the most optimal for preparation and analysis of activated carbons?

These were the questions that first of all needed to be answered in order to determine whether or not the algae derived activated carbon could be a possible replacement for the technologies for removal of sour gases. The following chapters will discuss the cultivation of algae, activation, and analysis of algae derived activated carbon materials.

CHAPTER 5

Cultavation of Microalgae Scenedesmus

This chapter describes how the microalgae Scenedesmus was cultivated. The algae was provided by AlgeCenter Danmark as described in section 2.2. The idea of this part of the project was to cultivate the algae and produce enough to make a sample of activated carbon with it. The properties of the microalgae were then to be compared to the macroalgae. It was chosen to test two different nutrients for the algae, normal liquid fertiliser used for plants and a special MWC/MWC-Se medium mixed as described in section 5.1.

5.1 Cultavation of Scenedesmus

Scadinavian Culture Collection of Algae and Protozoa has a database with different species of algae and how to make a media for them to live in. For the Scenedesmus genus the media is called MWC made by Guillard and Lorenzen in 1972 [27]. There were in total four different solution to be mixed.

5.1.1 1. Stock Solutions

Table 5.1 shows the six stock solutions [27]. Each were mixed individually in a flask with demineralised water using the quantities given in the table.

Table 5.1: 1. Stock solutions. [27]

Chemical	**Quantity**
$CaCl_2 \cdot 2H_2O$	3.68 $g/100\ mL$
$MgSO_4 \cdot 7H_2O$	3.70 $g/100\ mL$
$NaHCO_3$	1.26 $g/100\ mL$
$K_2HPO_4 \cdot H_2O$	1.14 $g/100\ mL$
$NaNO_3$	8.50 $g/100\ mL$
$Na_2O_3Si \cdot H_2O$	2.84 $g/100\ mL$

5.1.2 2. Trace Element Solution

Table 5.2 gives the chemicals and amount in the trace element solution [27]. For the trace element solution all elements in the table were mixed and demineralised water was added until a volume of 1000 mL was obtained.

Table 5.2: 2. Trace element solution. [27]

Chemical	**Quantity**
$Na_2EDTA \cdot H_2O$	4.36 g
$FeCl_3 \cdot H_2O$	3.15 g
$MnCl_2 \cdot 4H_2O$	0.18 g
H_3BO_3	1.00 g
1% $CuSO_4 \cdot 5H_2O$	1 mL
2.2% $ZnSO_4 \cdot 7H_2O$	1 mL
1% $CoCl_2 \cdot H_2O$	1 mL
0.6% $Na_2MoO_4 \cdot H_2O$	1 mL
dH_2O	to 1000 mL
The pH adjusted to 4-4.5 to retain the solubility of the metals	

5.1.3 3. Vitamin Primary Stock Solutions

Table 5.3 gives the chemicals and amounts in the vitamin stock solutions [27]. The two primary stock solutions were mixed individually following the ratio given in the table. When preparing the biotin solution add 9.6 mL of demineralised water per mg of biotin. For the solution of vitamin B_{12} add 0.89 mL of demineralised water per mg of B_{12} vitamin. Both were used on crystalline form.

Table 5.3: 3. Vitamin primary stock solutions. [27]

Chemical	**Quantity**
Biotin	0.01 $g/100\ mL$
Cyanocobalamin (B_{12})	0.01 $g/100\ mL$

5.1.4 4. Vitamin Stock Solution

For the second vitamin solution 20 mg of Thiamine HCl (Vitamin B_1) must be dissolved in approximately 80 mL of demineralised water in a 1000 mL volumetric flask [27]. Hereafter 1 mL of biotin primary stock solution must be added as well as 0.1 mL of the cyanocobalamin primary stock solution. Finally the flask must be filled with 100 mL of demineralised water. Hereafter the solution must be divided into 10 mL polyethylene vials and be frozen until it is to be used [27]. In this project the vitamin was just kept cool in a fridge.

5.1.5 Preparation of Medium

The medium consisted of 1 mL of stock solutions 1-6, 1 mL of the trace solution, and 0.5 mL of the vitamin mix. Either 115 mg of TES-buffer or 50 mL of 0.1% Tris-buffer. For this project TES-buffer was used. Then pH was adjusted to 7.5 [27]. Since the solution was acidic a base was added. In this project NaOH was used.

5.2 Startup

Approximately 900 mL of algae in a solution containing the soft water from a pig house was available. This amount was divided into two, 400 mL and 500 mL. The portion with 400 mL was mixed with 1 L of the MWC/MWC-Se medium described in section 5.1. The portion with 500 mL was mixed with 1 L of ordinary fertiliser, refer to appendix A for picture of bottle. Both mixtures were placed in a room with a fixed temperature of approximately 20 $°C$. A lamp was used to provide sufficient light as shown in figure 5.1. Furthermore, air was bubbled through the mixture while stirring. The cultivation was started the 9th of March 2016.

Figure 5.1: The two algae samples placed on a magnetic stirrer. A lamp provides light while air is bubbled through the samples. The sample to the left grows in the MWC/MWC-Se medium and the sample to the right grows in the universal fertiliser.

5.3 Observation of Algae Growth

The total growth of the algae is documented with photos in appendix A. After a week algae could be seen on the bottom of the flasks as shown in figure 5.2 The 16th of March 2016, one week after start, half a litre of nutrient was

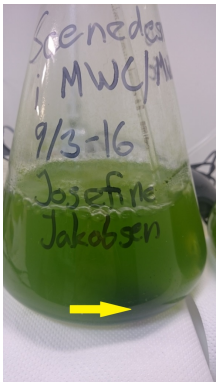

Figure 5.2: 15-03-16. Algae can clearly be seen at the bottom of the flask.

added to the two solution. MWC/MWC+Se to the one already containing the medium and universal fertiliser for the one already containing that. After two weeks a large portion of particles could easily be seen, specially in the

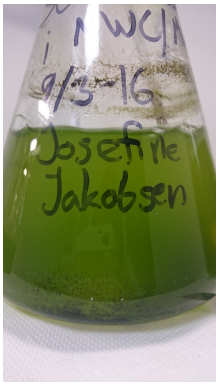

Figure 5.3: 06-04-16. Algae can be seen even more clearly now after one month.

solution containing the MWC/MWC+Se medium. The 30th of March 2016, three weeks after start, 0.25 L of nutrient was added to the two solution. MWC/MWC+Se to the one already containing the medium and universal fertiliser for the one already containing that. Once a week 0.25 L of nutrient was added to each flasks. After one month the growth of the algae could be observed in the flask as shown in figure 5.3. Generally the growth continued specially in the flaks containing the MWC/MWC+Se medium. The one containing the universal fertiliser became more and more yellow as shown in the pictures in appendix A. In the flask containing the MWC/MWC+Se medium the algae was growing in a way so the changes were easy to observe. It could from these observations be concluded that the algae material growing in the MWC/MWC+Se medium had the better growth.

5.4 Evaluation

At the beginning of the project period it was not one of the objectives to cultivate algae. Unfortunately only one litre of algae in a water solution was provided. It was attempted to take 100 mL of that and dry it to see the amount of dry matter. Unfortunately the amount was so small that it was clear that more had to be grown in order to have enough for an activated carbon sample. Therefore the test was initiated were the growth of the algae were compared between to different growth media. The reason for the use of the two different media was pure curiosity to see if there was any difference in the growth. This study showed that the tailored medium for the specific algae makes a positive difference in the growth. Even better growth would have been achieved by increasing the CO_2 level in the room as well as increasing the room temperature. The use of natural sunlight instead of lamps would probably increase the growth.

CHAPTER 6

Preparation of Activated Carbon

This chapter contains the procedure for preparation of algae derived activated carbon. The algae was activated using two chemical activation techniques. For the traditional chemical activation the influence of activation temperature and the ratio between activating agent and algae were explored in order to determine the optimal combination. Sulphuric acid can also be used as activating agent but the process is somewhat different. The outcome of the two methods was analysed in the next chapters.

6.1 Drying Fresh Macro Algae

For the main experiment the brown macro algae Fucus vesiculosus collected at a beach near Kolding was used. It was also planned to do some tests with the macroalgae collected at Esbjerg as well as the microalgae cultivated as described in chapter 5. This section mostly focus on the process using Fucus vesiculosus collected near Kolding, however the procedure for the other algae species are mostly the same.

As it was harvested directly from the sea the algae came in wet. Therefore the first step in the process was to wash and dry the algae. This was done in an oven at 80-90 $°C$ for at least 24 h as shown in figure 6.1. When all the water was evaporated, as shown in figure 6.2, the algae was crushed into smaller pieces as shown in figure 6.3. The dried algae was now ready for activation.

Figure 6.1: Fucus vesiculosus dried in an oven at 80 $°C$ for approximately 24 h.

Figure 6.2: Dried Fucus vesiculosus algae.

Figure 6.3: Dried and crushed Fucus vesiculosus algae.

6.2 Activation of the Algae Material Using Traditional Chemical Activation

In this section the procedure for the activation of the algae material, produced as described in section 6.1, will be presented. Since chemical activation was chosen it was necessary to choose an activating agent. For this project potassium hydroxide (KOH) was chosen since it has already proven its good abilities for chemical activation in other studies [17, 28, 29, 30, 31]. Table 6.1 shows

Table 6.1: Variables of the activation procedure.

Peak temperature [$°C$]	**KOH/algae ratio** [$-$]
600	1:1
700	2:1
800	3:1
900	

the variables of this process. As shown peak temperature and the ratio between KOH and algae were varied through different samples. From literature

it was indicated that preparation at temperatures between 800-900 $°C$ creates micropores where preparation at lower temperatures only creates mesopores. Therefore the activation should be performed using different temperatures in order to test this theory [26]. In total six different samples were prepared with the following parameters:

1. Temperature: 600 $°C$ and KOH/algae ratio: 2:1
2. Temperature: 700 $°C$ and KOH/algae ratio: 2:1
3. Temperature: 800 $°C$ and KOH/algae ratio: 2:1
4. Temperature: 900 $°C$ and KOH/algae ratio: 2:1
5. Temperature: 900 $°C$ and KOH/algae ratio: 1:1
6. Temperature: 900 $°C$ and KOH/algae ratio: 3:1

By preparing the samples this way it was possible to test how variations in activation temperature and KOH/algae ratio influenced the outcome. Please notice that six samples like sample 1-6 were prepared at Aalborg University by associate professor Vittorio Boffa. A version more of sample 1, 2, and 3 were also prepared at Aalborg University Esbjerg. For all tests three parameters were fixed:

- Temperature ramp up: Aalborg: 2 $\frac{°C}{min}$ and Esbjerg: 10 $\frac{°C}{min}$
- Nitrogen flow rate: Aalborg: 100 $\frac{cm^3}{min}$ and Esbjerg: 200 $\frac{cm^3}{min}$
- Activation time: 1 *hour*

6.2.1 Preparation of Powder Mixture

As KOH was used in solid form for activation the algae and KOH had to be mixed. In order to mix the solid algae and solid KOH both were ground together in a mortar. Similar for all samples were that in total 4 g of algae was used. The amount of KOH depended on the test performed. Hereafter the samples were ready for activation. The exact amount of the samples prepared by Vittorio Boffa is given in figure 6.2 in section 6.4.

6.2.2 Preparation in Furnace and Washing

The ceramic boat containing the algae/KOH mixture was placed in a tubular furnace. A schematic overview of a test setup is shown in figure 6.4. The figure shows that the setup for performing the activation procedure contained

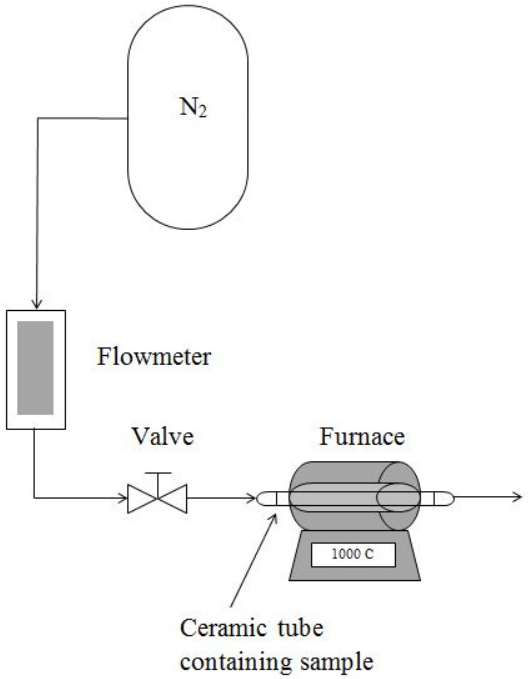

Figure 6.4: Schematic overview of an example of an activation test setup. [9]

a N_2 source, a flowmeter for controlling the gas flow, a valve to cut off the gas supply, and a furnace. After placing the sample in a ceramic boat in the furnace, the furnace was then cleaned for air using N_2 for 5-10 minutes. The flow of N_2 was then reduced to the desired flow. Setpoint temperature and heating rate was programmed. The system was now ready for run. The set-point temperature depended on the sample.

After the activation process the remaining KOH as well as reaction products were removed by as washing step. The samples were transferred to a beaker containing deionised water and left stirring overnight. Hereafter hydrocloric acid (HCl) was added to the samples in order to increase pH. Then the samples were centrifuged several times in steps. Between each step water was removed and replaced with new deionised water. Each step contained 5-30 minutes centrifugation. The process was repeated until the pH of the sample was approximately 7-8. Finally the samples were dried for 2 days at 90 $^{\circ}C$ in order to remove remaining water. The analysis of the carbon samples will be described in the next chapter.

6.3 Activation of Algae Material Using Sulphuric Acid

It was wanted to explore an alternative method to normal chemical activation. Therefore a method was found which did not include heating to more than 350 $°C$. For the preparation of algae in this section the specie Fucus Vesiculosus, described in section 2.1, was used.

6.3.1 Background

In studies presented by Esmaeili et al. [32, 33, 34] an alternative activation method was explored. For his method 97% pure sulphuric acid (H_2SO_4) was used in the ratio of 0.8 mL H_2SO_4 per gram of algae. The algae was kept in the solution for 24 h. Hereafter reflux was performed for 4 h. The solution was then cooled and washed several times with deionised water and it was soaked in 2% $NaHCO_3$ in order to remove the remaining acid. pH should hereafter be around 6-7. Finally the sample was dried in an oven at 150 $°C$ for 46 h.

6.3.2 Preparation

20 g of dried, crushed algae was added to 16 mL of 98 % pure H_2SO_4. It was observed that besides heat development the mixture expanded as shown in figure 6.5 and figure 6.6. The H_2SO_4 is known for its dehydrating abilities. When mixed with a compound containing sugar, such as plants, it will remove the water from the sugar and turn the material into a a porous carbon while developing heat and steam. The reaction was expected to be:

$$C_{12}H_{22}O_{11} + H_2SO_4 \rightarrow 12C + 11H_2O + H_2SO_4/H_2O \ \ mixture \tag{6.1}$$

The mixtures were left for almost four days. Hereafter the mixtures were heated in a digestion block as shown in figure 6.7 to 350 $°C$ since the boiling point of H_2SO_4 is 337 $°C$. This was done in order to remove some of the H_2SO_4 and support the reaction of removal of sugar from the algae. The samples were left there to the next day in order to cool down. The result of the removal of H_2SO_4 is shown in figure 6.8.

Figure 6.5: 17-03-16. Crushed, dried algae mixed with H_2SO_4.

Figure 6.6: 17-03-16. Crushed, dried algae mixed with H_2SO_4.

Figure 6.7: Samples containing dried, crushed algae and H_2SO_4 heated in a digestion block at 350 $°C$ for four hours.

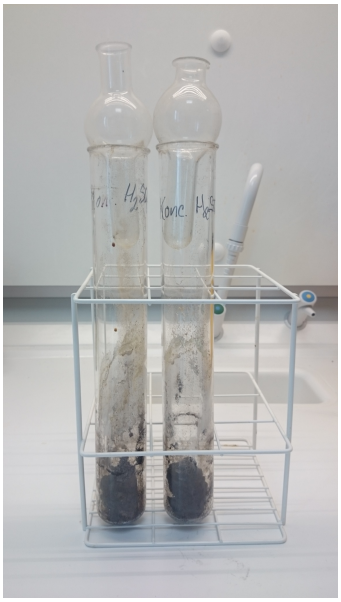

Figure 6.8: Algae samples after activation using H_2SO_4. The samples was washed in order to remove remaining acid.

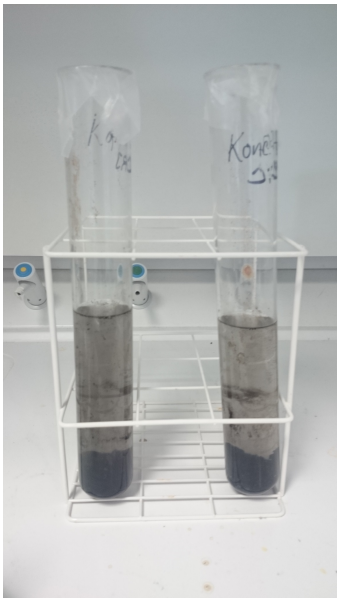

Figure 6.9: Washing of activated carbon from algae.

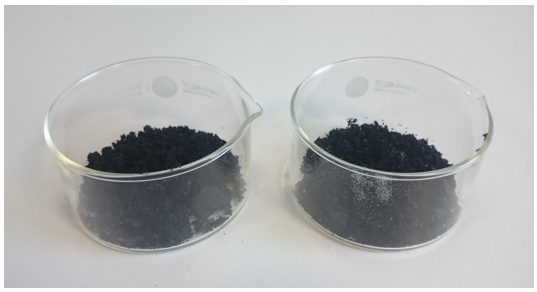

Figure 6.10: Activated carbon sampled after removal of water from washing.

Hereafter the samples were washed using deionised water in order to remove remaining acid. Deionised water was added to the sample as shown in figure 6.9. pH of the solution was checked and the water was removed. New water was added and again pH was checked. This sequence was repeated until a pH of 6 was reached. Approximately four washing steps were performed for each sample. It was noticed that no heat developed during the washing. This indicated that almost no H_2SO_4 was left with the sample.

When the pH of both samples were 6, water was filtrated from the sample and the solids were transferred to a small beaker as shown in figure 6.10. The samples were placed in an oven at 105 $^{\circ}C$ for a little more than 6 days in order to remove remaining moisture. After the drying process, the activated carbon

was ready to be tested. The analysis of the carbon samples will be described in the next chapter.

6.4 Analysis of Burn-Off of the Chemical Activation Procedure

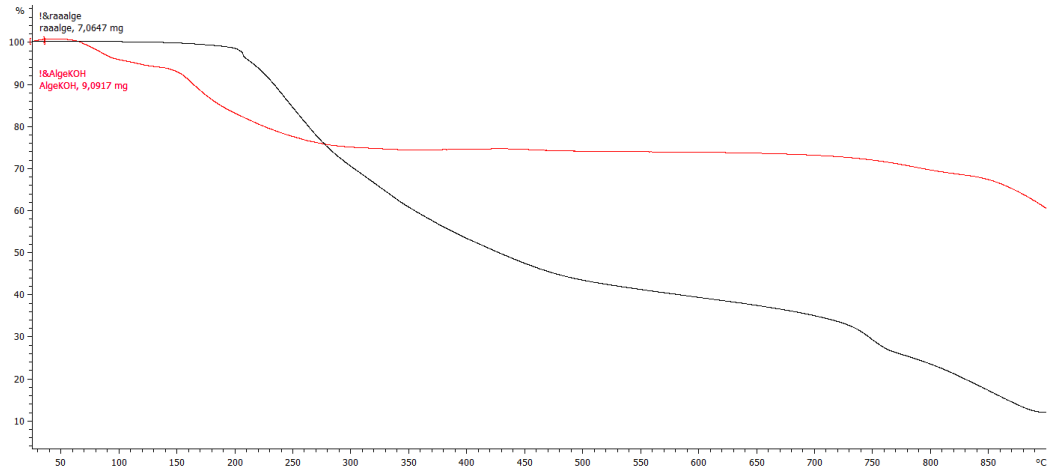

Figure 6.11: Thermogravimetric analysis of raw dried algae (black curve) and raw dried algae mixed with KOH (red curve).

A thermogravimetric analysis (TGA) was performed in order to determine how the activation process proceeds. The TGA was performed by weighing an amount of sample and placing it in the sample crucible. The program was set to heat from 25 $°C$ to 900 $°C$. The instrument measured the loss of mass of each increase in temperature. This was used to give an idea about the activation process. If for example most of the burn-off occurred at low temperatures, there would be no need to perform the activation at higher temperatures. However, the analysis could also reveal the need for using even higher temperatures. Figure 6.11 shows the TGA of raw dried algae (black curve) and raw dried algae mixed with KOH (red curve). The ratio between the KOH and the algae was 2:1. Figure 6.11 shows that for the raw dried algae at 900 $°C$ only a little more than 10 % ofthe original mass was left. However for the algae mixed with KOH approximately 60 % of the original mass was left. The question is then if the mass lost created pores or not. And if, which kind. To explore this, different equipment must be used. In this project different samples were analysed based on their surface area and pore size distribution using the BET and BJH theory as described in chapter 7.

Table 6.2: Mass of samples prepared by Vittorio Boffa before and after activation. The first row contains the sample name, the temperature of which it was prepared, the ratio between KOH and algae and the unit.

	Sample 1 600 2:1 $[g]$	Sample 2 700 2:1 $[g]$	Sample 3 800 2:1 $[g]$	Sample 4 900 2:1 $[g]$	Sample 5 900 1:1 $[g]$	Sample 6 900 3:1 $[g]$
Before activation	11.0861	11.8372	11.7365	11.4268	7.4833	15.4649
After Activation	9.1193	9.0055	8.5452	8.4531	4.0584	11.5752

The conclusion to this analysis is that it is expected that the burn-off is constant for all samples prepared with the same KOH/algae ratio.

Table 6.2 the mass of the samples prepared by Vittorio Boffa before and after activation. As also indicated by the TGA, the burn-off was constant for the samples with the same starting mass and KOH/algae ratio. According to figure 6.11 approximately 70 % of the original mass ought to be retained. For all samples but sample 5 the percentage retained was approximately 70 %. For sample 5, the amount retained was only 50 %. This result is also supported by the results from the TGA in figure 6.11 which showed that the burn-off is much higher for the sample without any KOH compared to the sample with the KOH/algae ratio of 2:1. What can be concluded from this is that more mass is retained if KOH is added to the sample. As described in chapter 2 the main component in the algae is cellulose. Therefore a test was initiated similar to the TGA of the algae material in order to investigate if it was the cellulose of the algae which created the outcome of the test. The results of that test is shown in figure 6.12. The figure shows to be almost identical to that of the algae. Without KOH almost all of the algae is combusted during the process. By adding KOH in a KOH/cellulose ratio of 2:1 approximately 70% of the original mass was retained. The same as for the algae material. This confirmed the theory that it was the cellulose of the algae which reacted with the KOH in order to form an even stronger material. A study by Van Loon et al. [35] supports these results. A peeling-off reaction was proposed where in the beginning of the reaction glucose units were peeled of from the cellulose in the presence of heating and and OH^- group. The process stops again by it self do to a reduction of the end groups. The stopping mechanism is divided into chemical stopping and physical stopping [35]. The end groups are transformed into the crystalline region which are not accessible to alkali [35].

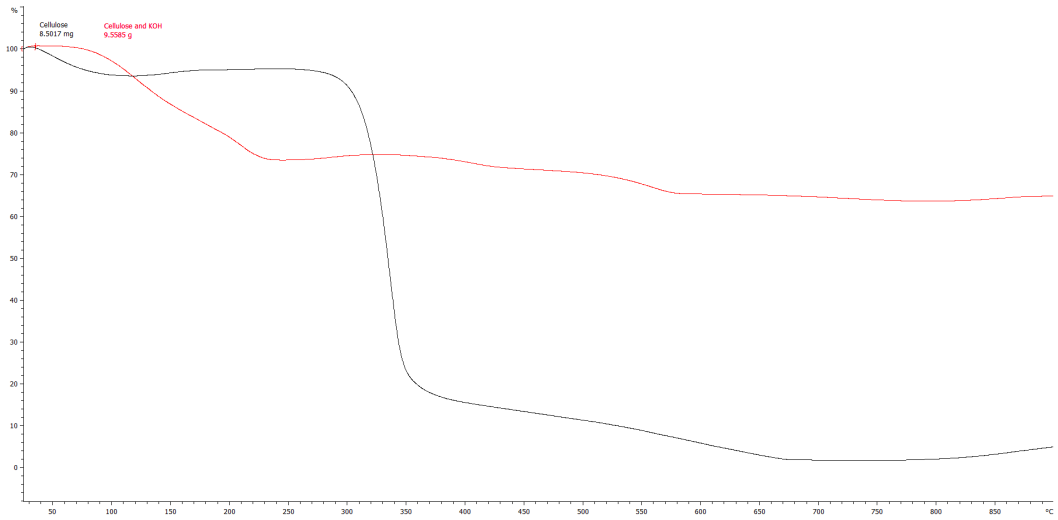

Figure 6.12: Thermogravimetric analysis of cellulose (black curve) and cellulose mixed with KOH (red curve).

This could be a reasonable explanation for the phenomena shown in the two figures. However, more tests should be performed and compared to relevant or similar studies in order to propose a final explanation.

6.5 Evaluation

When the project period started it was discovered that the plugs used for the furnace were lost as the furnace was moved to a new lab. The furnace had not been used for high temperatures for a long time and therefore the need for high temperature plugs had not been there. Naturally new plugs were ordered. Unfortunately it was not a stock item at the Danish dealer and it had to be ordered from the manufacturer in The United States of America. A period of approximately three months went by before the plugs arrived in the end of May. Several times the delivery date was postponed. In the beginning of May six samples were sent to Vittorio Boffa at Aalborg Univeristy for him to prepare the samples. At this point already at lot of time went by without the possibility to prepare or analyse any samples. This was a highly unfortunate situation which maybe could have been avoided if preparation for the project was initiated earlier. This was however a good learning process where the conclusion was to check the need for and order spare parts in good time.

The whole process of activated carbon production from an organic source is a time consuming process. Using conventional chemical activation takes one to two days to dry the algae material, half day to prepare it in the furnace, one

and a half day of washing, and finally two days of drying. This means that one sample can easily take five days from start to finish to prepare. This makes the process very time consuming which could be a problem if the method was tried to be commercialised. Perhaps the method should be tested with a higher heating rate and shorter preparation time in the furnace. This could maybe cut down the preparation time with some hours. Also the washing step could be shortened by studying the exact amount of acid needed to neutralise the sample after the pyrolysis. Furthermore by using a vacuum oven instead of a traditional oven at lot of time could be spared in the two drying phases. Combining all these initiatives the preparation time of one sample could maybe be reduced to two days.

CHAPTER 7

Analysis of Surface Area of Activated Carbon

For the analysis of the surface area of the prepared activated carbon from chapter 6 the BET theory was used. The sample was analysed by a ThermoQuest Sorptomatic 1990 instrument that utilises the BET equation.

For the program the density of the algae was set to 1.36 $\frac{g}{mL}$. The purpose of the tests was to investigate the surface area of the algae before and after activation.

7.1 Operational Procedures

The method of the machine used in this project was simple gas adsorption manometry. Gas was discontinuously injected stepwise until an equilibrium was obtained. Hereafter the amount of adsorbed material could be calculated from the change in pressure. The following subsections describe the procedures and important parameters.

7.1.1 Sample Mass

After the mass of a degassed sample burette was measured the sample was added. The choice of amount of sample mass had a great influence on the analyses. For a low surface area material a large quantity should be used. For example for a material with extremely low surface area, e.g. 1 $\frac{m^2}{g}$, 10 g should be a appropriate amount for the analysis [26]. However, it was also necessary to be careful not to choose a mass too little in the case of high surface area. There are two reasons for that; the sample must be representative for the entire

batch as well as the accuracy of the measured mass must reflect the accuracy of the adsorption measurement [26].

7.1.2 Outgassing

After measuring the mass of the burette containig the sample the system was outgassed and yet again the mass of the system was measured. Subtracting the mass of the burette from the mass of the total system it was possible to calculate the mass of the sample without any thing adsorbed onto it. The outgassing procedure was performed by slowly introducing a vacuum to the system while the sample burette was placed in a furnace. The temperature depended on the sample type, organic materials only requires a temperature of 60-70 $°C$ while highly porous materials such as activated carbons requires approximately 240 $°C$. If the sample is a powder, as it was in this project, certain caution must be applied in order for the powder not to be sucked up by the vacuum pump. However, this does not necessarily produce a perfectly clean surface [26]. In many cases this is also not needed as the material was tested for usage outside the lab where exposure to atmospheric conditions would be almost inevitable. This leads to the real aims of the outgassing procedure [26];

1. remove physiosorbed species from the material, e.g. CO_2 and H_2O,

2. avoid agering or modification of functional groups, and

3. reach a reproducible intermediate state.

7.1.3 Analysis

For the analysis the degassed burette containing the sample was placed in a small dewar with liquid nitrogen. Liquid nitrogen was used in order to assure a stable temperature of -196 $°C$ throughout the test. Variations in temperature could cause dramatic changes in pressure. A 0.1 $°C$ change in temperature could cause a 10 $mbar$ pressure change [26]. Stepwise N_2 was injected into the sample burette. When equilibrium was achieved the amount of adsorbed N_2 was calculated. This was done until the complete adsorption isotherm was produced. Hereafter desorption was performed in the same manner in order to produce the desorption isotherm. The method of the calculations was the BET theory.

7.2 BET Theory

The Brunauer-Emmett-Teller (BET) theory is used to determine the surface area of porous materials. The theory was proposed by Stephen Brunauer, Paul Hugh Emmett, and Edward Teller in 1938. It is important to state that the surface area calculated using the BET theory is not the absolute surface area and must not be compared to the surface area of materials calculated with other methods. The method is based on the theory proposed by Langmuir where M is defined as the number of adsorption sites. The first filled site is denoted M_1 and the bare sites are M_0. This means that as the number of adsorbed sites increases the number of bare sites decreases meaning that both of them are varying throughout the process. By calculating $M - M_1$ can be used to define M_0. For now only the formation of a monolayer is considered. Defining the rate of adosorption as [36]:

$$R_a = k_a P M_0 \tag{7.1}$$

The rate of desorption can then be defined as [36]:

$$R_{d,1} = k_{d,1} M_1 \tag{7.2}$$

Here the subscript 1 refers to that it is the first layer that is considered.
At equilibrium the two rates must be equal:

$$k_a P M_0 = k_{d,1} M_1 \tag{7.3}$$

As the adsorption is restricted to the monolayer only the total number of sites is [36]:

$$M = M_0 + M_1 \tag{7.4}$$

By isolating M_0 in equation 7.4 and inserting into equation 7.3 gives the Langmuir equation [36]:

$$\begin{aligned} k_a P(M - M_1) &= k_{d,1} M_1 \\ &\Updownarrow \\ \frac{k_a}{k_{d,1}} P &= \frac{M_1}{M - M_1} \end{aligned} \tag{7.5}$$

k_a is the rate constant of adsorption while $k_{d,1}$ is the rate constant of desorption of the first layer. The rate of desorption is a result of the interactions between the adsorbate and the adsorbent. The rate of desorption is proportional to a frequency factor, ν, and the energy of adsorption, ε, and the Boltzmann factor, k_B [36]:

$$k_{d,1} \propto \nu \cdot exp\left(-\frac{\varepsilon}{k_B T}\right) \tag{7.6}$$

Observing equation 7.6 its relation to Arrhenius' equation is evident. The main difference is that the activation energy of Arrhenius' equation is switched with the energy of adsorption. The frequency factor is used to describe the frequency of the adsorption.

Moving on from only exploring the properties of the monolayer to looking at the development of a multilayer too. First equation 7.4 can be modified to work for all possible layers from 0 to n. The thickness is of i molecules. The equation becomes:

$$M = M_0 + M_1 + M_2 + ... + M_n = \sum_{i=0}^{n} M_i \tag{7.7}$$

Using the same analogy as in equation 7.1 for the second layer it is possible to define the rate of adsorption of that layer. The rate constant is assumed to be the same. The new rate of the second layer is [36]:

$$R_a = k_a P M_1 \tag{7.8}$$

The desorption from the second layer can be defined using the same analogy as in equation 7.2. The rate of desorption from the second layer is:

$$R_{d,2} = k_{d,2} M_2 \tag{7.9}$$

The rate constant $k_{d,2}$ is assumed to be on the same form as in equation 7.6. However, there is an important difference. The desorption from the first layer is from the adsorbent where for the outer layers the desorption is from another adsorbate. This implies that a modification must be made. Replacing the energy of adsorption (or desorption), ε, in equation 7.6 with the energy of vaporisation, ε_V the new rate constant can be defined as:

$$k_{d,2} = \nu \cdot \exp\left(-\frac{\varepsilon_V}{k_B T}\right) \tag{7.10}$$

Similar to the consideration of the monolayer, at equilibrium the rate of adsorption is equal to the rate of desorption:

$$k_a M_1 P = k_{d,2} M_2 \tag{7.11}$$

It is assumed that the activation energy of desorption is equal for all the outer layers. Therefore equation 7.11 can be rewritten in order to generalise it for all outer layers where $2 \leq i < n$ [36]:

$$k_a M_{i-1} P = k_{d,i} M_i \tag{7.12}$$

It is wanted to relate the current layer, M_i, with the previous layer, M_{i-1}. M_i can be related to M_0 using equation 7.3:

$$M_i = \left(\frac{k_a}{k_{d,i}}P\right)^{i-1} M_{i-(i-1)} = \left(\frac{k_a}{k_{d,i}}P\right)^{i-1} M_1 = \left(\frac{k_a}{k_{d,i}}\right)^{i-1} \frac{k_a}{k_{d,1}}P^i M_0 \quad (7.13)$$

As previously mentioned k_a is constant while $k_{d,i}$ only changes in Boltzmann factor. Knowing this, equation 7.13 can be rewritten to:

$$M_i = \frac{k_a^i P^i M_0}{\nu^i (exp(-\varepsilon_V/k_B T))^{i-1} \cdot exp(-\varepsilon(k_B T)} \quad (7.14)$$

Multiplying the nominator and denominator by $(-\varepsilon_V/k_B T)$ and implementing that $x^{i-1} \cdot x^1 = x^i$ gives:

$$\begin{aligned} M_i &= \frac{k_a^i P^i M_0}{\nu^i (exp(-\varepsilon_V/k_B T))^{i-1} \cdot exp(-\varepsilon(k_B T)} \cdot \frac{exp(-\varepsilon_V/k_B T)}{exp(-\varepsilon_V/k_B T)} \\ &\Updownarrow \\ M_i &= \frac{k_a^i P^i M_0}{\nu^i (exp(-\varepsilon_V/k_B T))^{i}} \cdot \frac{exp(-\varepsilon_V/k_B T)}{exp(-\varepsilon/k_B T)} \end{aligned} \quad (7.15)$$

Two values, x and C, are introduced in order to combine some properties:

$$M_i = x^i C M_0 \quad (7.16)$$

Defining the properties x and C. x can be defined using equation 7.10

$$x^i = \frac{k_a P}{\nu \cdot exp(-\varepsilon_V/k_B T)} = \frac{k_a}{k_{d,i\geq 2}}P \quad (7.17)$$

Hereafter C can be defined as:

$$C = exp\left(\frac{\varepsilon - \varepsilon_V}{k_B T}\right) \quad (7.18)$$

Please notice that only a positive value of C has a physical meaning. Inserting equation 7.16 into equation 7.7 gives:

$$M = M_0 + \sum_{i-1}^{n} x^i C M_0 \quad (7.19)$$

The volume of the formed monolayer is used to define the available surface area of the porous material. The volume of the monolayer, V_m, is compared to the volume adsorbed, V, in order to determine the surface area. Since M_i is the number of sites with a given depth, i, then by timing the number of sites for the specific depth together with the depth the volume can be found.

By doing this for all sites and adding them together the total volume can be estimated [36]:

$$V = \sum_{i=1}^{n} V_i \propto \sum_{i=1}^{n} iM_i \tag{7.20}$$

The volume of the monolayer is proportional to the total number of sites [36]:

$$V_m \propto M = M_0 + \sum_{i=1}^{n} M_i \tag{7.21}$$

Here i is not included since we are only interested in the volume of the monolayer. The ratio between equation 7.20 and equation 7.21 eliminates the unknown proportionality factor:

$$\frac{V}{V_m} = \frac{\sum_i iM_i}{M_0 + \sum_i M_i} \tag{7.22}$$

Combining equation 7.16 with equation 7.22 results in:

$$\frac{V}{V_m} = \frac{C\sum_i ix^i}{1 + C\sum_i x^i} \tag{7.23}$$

The expression $\sum_i x^i$ can be defined as a power series [36]:

$$\sum_i x^i = x(1 + x + x^2 + ...) = x(1 - x)^{-1} \tag{7.24}$$

The expression $\sum_i ix^i$ can be rewritten as a differential equation [36]:

$$\sum_i ix^i = x\sum_i ix^{i-1} = x\left(\frac{d}{dx}\right)\sum_i x^i \tag{7.25}$$

Inserting equation 7.24 into equation 7.25 gives:

$$\sum_i ix^i = x\frac{d}{dx}(x(1 - x)^{-1}) = \frac{x}{(1 - x)^2} \tag{7.26}$$

Finally equation 7.24 and equation 7.26 are inserted into equation 7.23. This gives the BET equation:

$$\frac{V}{V_m} = \frac{C\frac{x}{(1-x)^2}}{1 + C\frac{x}{(1-x)}} = \frac{Cx}{(1 - x)(1 + (C - 1)x)} \tag{7.27}$$

By observing equation 7.27 it is realised that as $V \to \infty$ then $x \to 1$. This will happen when $P \to P_0$. Combining this with equation 7.17 gives that:

$$1 = \frac{k_a}{k_{d,i\leq 2}} P_0 \tag{7.28}$$

Therefore x can also be defined from the relative pressure only:

$$x = \frac{P}{P_0} \tag{7.29}$$

Inserting equation 7.29 into equation 7.27 gives to most common version of the BET equation:

$$\frac{V}{V_m} = \frac{C(P/P_0)}{(1-(P/P_0))(1+(C-1)(P/P_0))} \tag{7.30}$$

The BET equation is often used on its linear form:

$$\frac{(P/P_0)}{V(1-(P/P_0)} = \frac{1}{C \cdot V_m} + \frac{(C-1)(P/P_0)}{C \cdot V_m} \tag{7.31}$$

The linear version of the BET equation is the one used to determine the surface area. The left side is plotted with $\frac{1}{V(1-(P/P_0)}$ against (P/P_0) in order to determine V_m. The plot is mostly linear in the relative pressure range of 0.05-0.3 [37]. Below the range the BET equation underestimate the value of V_m and above the range the equation overestimate the value [36]. Therefore the volume of gas corresponding to the coverage of a monolayer can be determined as:

$$V_m = \frac{1}{Slope + Intercept} \tag{7.32}$$

The constant C from equation 7.18 can be determined as:

$$C = \frac{Slope}{Intercept} + 1 \tag{7.33}$$

It is very important to calculate C since it helps to determine whether the surface area has a physical meaning or not. A high C value indicates that the adsorption energy is high [25]. Hammond et al. [25] claim that an optimal value of C is found between 50 and 200. Figure 7.1 shows an illustration of the BET plot with V/V_m as a function of both relative pressure P/P_0 and the constant C. It is shown that the shape of the curves change as the value of C is increased. Furthermore it shows that at the relative pressure increases the volume of the adsorbed layer increases.

Only observing the monolayer V must be equal to V_m. This means that the left side if equation 7.30 can be replaced by 1:

$$1 = \frac{C(P/P_0)}{(1-(P/P_0))(1+(C-1)(P/P_0))} \tag{7.34}$$

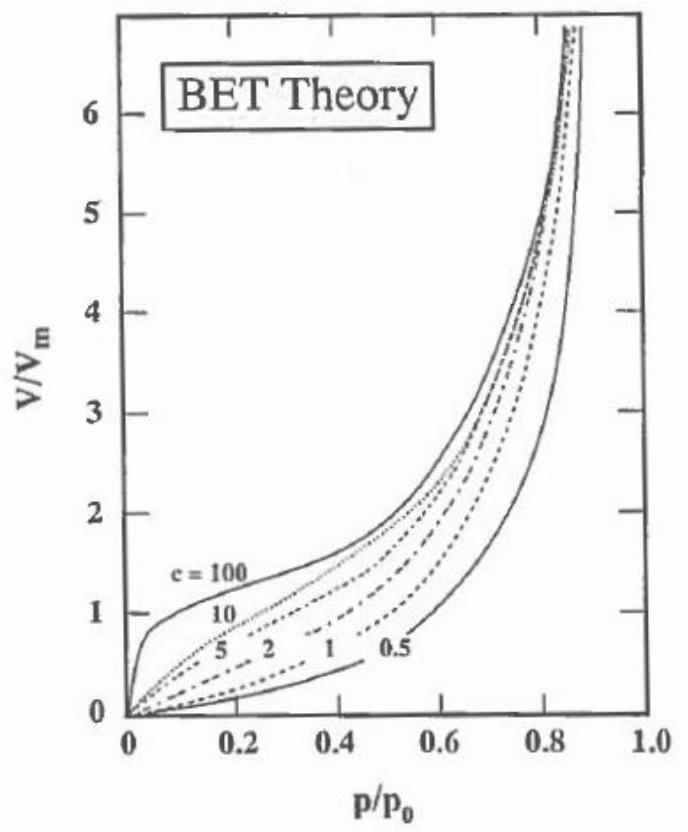

Figure 7.1: Illustration of the variation of the BET plot for V/V_m as a function of P/P_0 and C. [36]

Rewriting this equation:

$$\begin{aligned}
(1-(P/P_0))(1+(C-1)(P/P_0)) &= C(P/P_0) \\
1-(P/P_0)+(1-(P/P_0))(C-1)(P/P_0) &= C(P/P_0) \\
1-(P/P_0)+(C-C(P/P_0)-1+(P/P_0))(P/P_0) &= C(P/P_0) \\
1-(P/P_0)+C(P/P_0)-C(P/P_0)^2-(P/P_0)+(P/P_0)^2 &= C(P/P_0) \\
1-C(P/P_0)^2+(P/P_0)^2 &= 0 \\
1-2(P/P_0)+(P/P_0)^2(1-C) &= 0 \\
1-2(P/P_0) &= (P/P_0)^2(C-1)
\end{aligned} \tag{7.35}$$

At the monolayer (P/P_0) is very small which means that the expression $1-2(P/P_0)$ can be approximated to be 1. Applying that to the equation:

$$\begin{aligned}
(P/P_0)^2(C-1) &= 1 \\
(P/P_0)^2 &= \frac{1}{C-1} \\
(P/P_0) &= \frac{1}{\sqrt{C-1}}
\end{aligned} \tag{7.36}$$

This equation can be used to relate the relative pressure of the monolayer with the C value. This equation is only applicable for C values larger than 1. A similar equation is given by Jean et al. [26]. From equation 7.30 it is given that the relative pressure corresponding to the monolayer capacity is depending on the value of C given from [26]:

$$\left(\frac{P}{P_0}\right)_{V_m} = \frac{1}{\sqrt{C}+1} \tag{7.37}$$

This is equation is very similar to equation 7.36. The difference is found on the right side where the square-root is now only of the C value and 1 has changed from minus to plus. It is not stated by Jean et al. [26] how they got to that equation. The simmilarities to equation 7.36 are evident however the differences are rather significant. The equation be Jean et al. [26] is not restrained to only using C values above 1. At very high C values the differences of the two equations will not be as easy to spot in the outcome of the equations. However, at low C values the differences would be much more significant.

From equation 7.18 it is given that a high adsorption energy equals a high C value. From equation 7.37 it is shown that a high C values gives a low relative pressure corresponding to the monolayer capacity. This gives a very well-defined B point given from figure 3.4 and as shown in figure 7.1. In figure 7.1 it is clear that a higher C value gives a much clearer view of the B point compared to low C values. This leads on to another feature of the C value. Using the BET equation it is possible to predict the surface covered with the statistical monolayer and thereby predict the fraction of the surface that is still uncovered [26]. This fraction is directly dependent on the C value [26]:

$$(\theta_0)_{V_m} = \frac{1}{\sqrt{C}+1} \tag{7.38}$$

From equation 7.38 it is given that a a high value of C gives that the fraction of uncovered surface area is smaller. Connecting equation 7.37 with equation 7.38 gives a relation between the relative pressure and the fraction of uncovered surface area:

$$(\theta_0)_{V_m} = \left(\frac{P}{P_0}\right)_{V_m} \tag{7.39}$$

According to Jean et. al. [26] point B of figure 3.4 can be connected to the point of which the system changes from monolayer adsorption to multilayer adsorption. Therefore the relative pressure at point B can be inserted into equation 7.39 in order to find the fraction of uncovered surface.

Table 7.1: Molecular areas of adsorptives. [26]

Adsorptive	T $[K]$	Cross-sectional area σ $[nm^2]$		
		Literature range	In close-packed liquid minilayer	Customary value
Nitrogen	77	0.13-0.20	0.162	0.162
Argon	77	0.10-0.19	0.138	0.138
Krypton	77	0.14-0.24	0.152	0.202
Xenon	77	0.16-0.25	0.168	0.170
Oxygen	77	0.13-0.20	0.141	0.141
Carbon dioxide	195	0.14-0.22	0.163	0.210
n-Butane	273	0.32-0.53	0.321	0.430
Benzene	293	0.25-0.51	0.307	0.430

However, the volume of the adsorbed monolayer does not directly say anything about the surface area. Therefore the value of the adsorbed monolayer must be converted into a specific surface area using [36]:

$$SA_{BET} = \frac{V_m N_a \sigma^0}{M_V} \tag{7.40}$$

Where the input data when using N_2 are [36]:

- N_a is Avogadro's number: $6.02 \cdot 10^{23}\ mol^{-1}$
- σ^0 is the adsorption cross section of the adsorbate N_2: $1.62 \cdot 10^{-19}\ m^2$
- M_V is the molar volume of the adsorbate gas: $22,400\ \frac{m^3}{mol}$ at STP

Table 7.1 shows the cross-sectional area of a variety of adsorptives. It is shown that the difference is quite significant. Especially close to or at the surface of the adsorbent the morphology of the adsorbate can have some influence. Further away from the surface the influence of morphology of the specific material is less significant. For most adsorption experiments N_2 is used, however to get a better idea of the true nature of the surface of a material several different gases should be used for identical adsorption experiments.

7.3 Pore Size Distribution

A theory for calculating the pore size distribution was proposed by Dollimore and Heal which is and refined version of the method proposed by Elliot P. Barret, Leslie G. Joyner and Paul P. Halenda [26, 38].

When using the method it is assumed that [26];

- for the complete mesopore range the Kelvin equation is applicable:

$$ln\left(\frac{P}{P_0}\right) = -\frac{2\lambda V^l}{r_K RT}$$

  where:

  - λ is the surface tension,
  - V^l is the volume of the liquid,
  - r_K is the mean radius of the curvature of the meniscus,
  - R is the ideal gas constant, and
  - T is the temperature.

- the curvature of the meniscus is controlled by the pore size and shape.
- all pores are rigid and has a well-defined shape,
- only mesopores are present,
- the location of the pore does not have an influence on the process, and
- adsorption on pore walls and on open surface proceeds in the same way.

The pore size distribution is analysed as the desorption process is performed. This means that surface area and pore size distribution can be analysed at the same time. The first step in desorption is the removal of capillary condensate [26]. Hereafter the desorption involves removal of condensate from cores and thinning of the multilayer [26]. In this section the suffix K indicates that it is about the inner core and p indicates that it is about the pore. The nitrogen removed from each desorption step, "'j"', is in mole $\delta n(j)$ and as a volume $\delta V^l(j)$ of liquid nitrogen. For the first step ($j = 1$) the entire desorption is from capillary evaporation [26]. This means that the volume of core space released is equal to the volume of nitrogen removed [26]:

$$\delta V_K(1) = \delta V^1(1) \tag{7.41}$$

Assuming cylindrical pores, for the first and largest group of mesopores the core volume and pore volume can be related:

$$V_p(1) = \frac{\overline{r}_p^2(1)}{\overline{r}_K^2(1)} V_K(1) \tag{7.42}$$

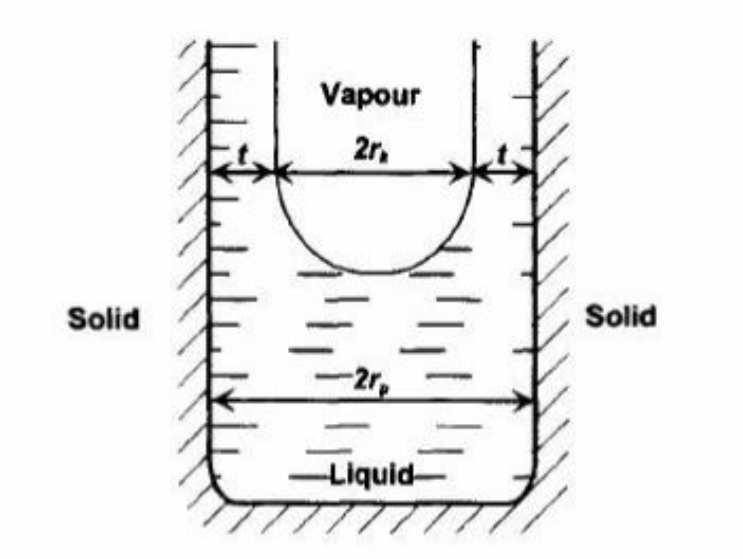

Figure 7.2: Illustration of the location of the pore and core radii. [26]

where $\overline{r}_p^2(1)$ and $\overline{r}_K^2(1)$ are the mean pore and core radii in the first step. These two radii are illustrated in figure 7.2. The figure also illustrate the total pore volume as well as the core volume.

After the first step the contribution from the thinning of the multilayer thickness, $\delta t(j)$ must be considered for the step j [26]:

$$\delta V(j) = \delta V_K(j) + \delta V_t(j) \tag{7.43}$$

where $V_K(j)$ is the emptied core volume from step j and $\delta V_t(j)$ is the removed equivalent liquid volume from the multilayer thickness. For the volume, $\delta V(j)$, in step j the group of pores emptied of condensate can be calculated as [26]:

$$\delta V_p(j) = \frac{\overline{r}_p^2(j)}{(\overline{r}_K(j) + \delta t(j))^2} \cdot \delta V_K(j) \tag{7.44}$$

where $\overline{r}_p^2(j)$ and $\overline{r}_K(j)$ is the mean pore and core radii of the step j. Using equation 7.42, 7.43, and 7.44 it is possible to obtain all the successive contributions to the total pore volume, $\delta V_p(1)$, $V_p(1)$,..., $\delta V_p(j)$ [26]. However it is necessary first to know the individual values for each stage of a stepwise procedure, $\delta_l(j)$. The core area can be defined as [26]:

$$\delta a_K(j) = 2\frac{\delta V_K(j)}{\overline{r}_K(j)} \tag{7.45}$$

and the pore are can be defined as [26]:

$$\delta a_p(j) = 2\frac{\delta V_p(j)}{\overline{r}_p(j)} \tag{7.46}$$

These areas area related with the equation [26]:

$$\begin{aligned} \delta a_K(j) &= \delta a_p(j) \frac{\overline{r}_p(j) - \overline{t}(j)}{\overline{r}_p(j)} \\ &= \delta a_p(j) \cdot \rho(j) \end{aligned} \tag{7.47}$$

According to the original BJH method the correction factor, $\rho(j)$, is only a single value corresponding to the most frequent pore size. The total pore volume and area by adding all the contribution from the different steps together.

The method proposed by Dollimore and Heal is very similar to the BJH theory. However $\delta V_P(j)$ is defined in a different manner [38]:

$$\begin{aligned} \delta V_p(j) &= \frac{\overline{r}_p^2(j)}{\overline{r}_K^2(j)} V_K(j) \\ &= \frac{\overline{r}_p^2(j)}{\overline{r}_K^2(j)} \left(\delta V(j) - \delta t \sum_j S_p + 2\pi t(j) \sum L_p \right) \end{aligned} \tag{7.48}$$

where:

- S_p is the specific are of the pore: $S_p = 2\frac{\delta V_p}{r_p}$, and
- L is the pore length.

In reality there is no need to calculate the pore length since the length and the specific area can be related as [39]:

$$2\pi L_p = \frac{S_p}{r_p} \tag{7.49}$$

7.4 Results

The section features the adsorption-desorption curves of the different experiments including the pore size distributions. All the results are for samples prepared at Aalborg Univeristy Esbjerg.

In table 2.2 and figure 3.9 values are reported of surface area of different activated carbons. From a previous study [9] using a microalgae but the same activation technique the highest achieved surface area was approximately 1500 $\frac{m^2}{g}$. Therefore it was expected to achieve surface area within the range of 1000-2000 $\frac{m^2}{g}$. However, to make sure that the large surface area was created from activation the surface area of the raw dried algae also had to be tested. The surface area of commercially available activated carbons are around 1500 $\frac{m^2}{g}$, therefore the goal of this project was to achieve an activated carbon material

with a slightly higher surface area.

As the theory was that high temperatures create micropores the pore size distribution should be different between the different samples. This theory was supported by a previous study [9] which indicated that the percentage of micropores increased with temperature. The non-activated sample should not contain many micropores while the one prepared at the highest temperatures should contain the most. Just to remind that micropores are more suited for adsorption of small molecules such as CO_2 and H_2S since they can easily escape the larger meso- and macropores.

The software for the BET instrument had several options for setup, some setups were suited for mesoporosity, high porosity, and low porosity. The difference between the different setup were the amount of data points desired, the equilibrium deviation meaning the amount the equilibrium pressure may deviate through a time period in order for it to register as a point.

7.4.1 Non-activated Algae

This section contains the results of the surface area and pore size distribution analysis for raw dried algae material. This sample was tested using a software setup for low porosity materials.b Figure 7.3 shows the adsorption and desorption isotherm for raw dried algae of the specie Fucus vesiculosus collected from a beach near Kolding. The shape of the curve indicates that this is a type IV isotherm as described and shown in section 3.3.1. The curve has an s-shape with a hysteresis loop indicating mesoporosity according to figure 3.7. The increase in adsorption at low relative pressures is too small for it to indicate microporosity. Also comparing with figure 3.8 the hysteresis loop of this sample was of type H3 indicating slit-shapes pores. The BET surface area of this sample was 20 $\frac{m^2}{g}$ with a C value of 176. This is a very high C value, however it is still acceptable as it is not negative. Comparing to figure 7.1 the shape of the adsorption isotherm should have a s-shape as it is the case for figure 7.3. All of this indicates that dried non-activated macroalgae is has a natural porosity. However the surface area is too small to use it in its natural from as an adsorption material. Therefore activation was required.

Figure 7.4 shows the pore size distribution of the raw algae material. The figure shows that the material naturally has a low amount of micropores. However most of the pores are located in the mesoporous and macroporous region. This type of distribution is highly unwanted for adsorption of small molecules such as CO_2 and H_2S. How the distribution is mesoporous compared to macro-

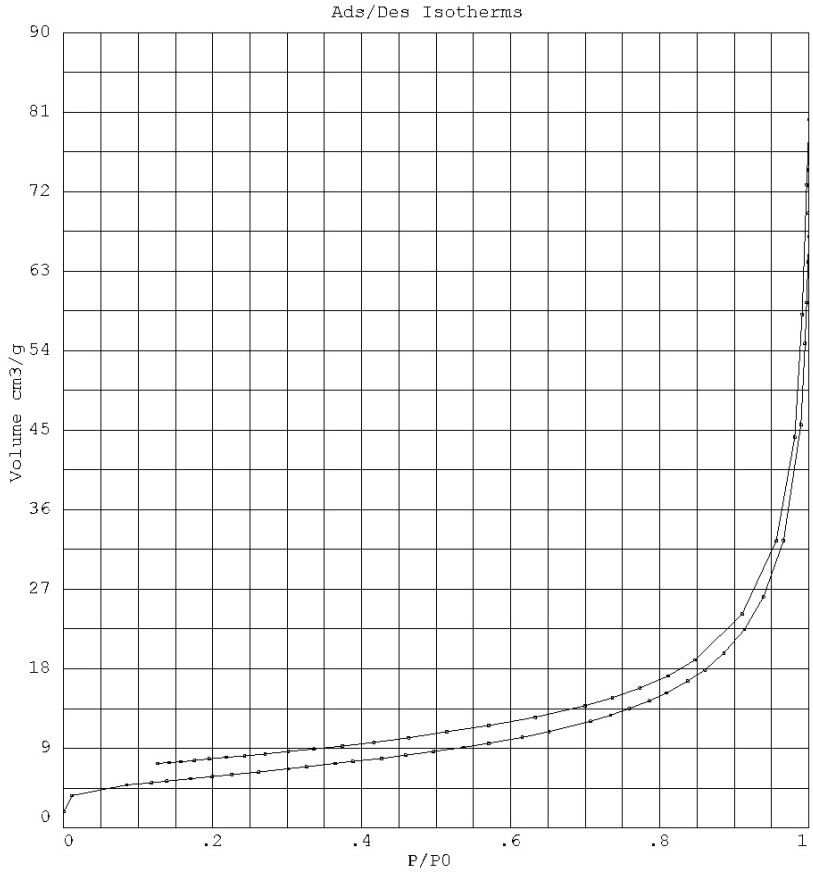

Figure 7.3: Adsorption-desorption isotherm of N_2 at -196 $°C$ on raw dried algae of the specie Fucus vesiculosus collected from Kolding.

porous cannot be determined from these results. However since the percentage of microporosity is the most vital part of this project it was not considered to be a problem. Notice that the desorption isotherm is not completely finished in this experiment. In order for it to be completed it should reconnect with the adsorption isotherm. This is a fault of the setup of the program and more point should have been used. However, it is not a significant issue since it is clear that there is an hysteresis loop which indicated the mesoporosity of the material.

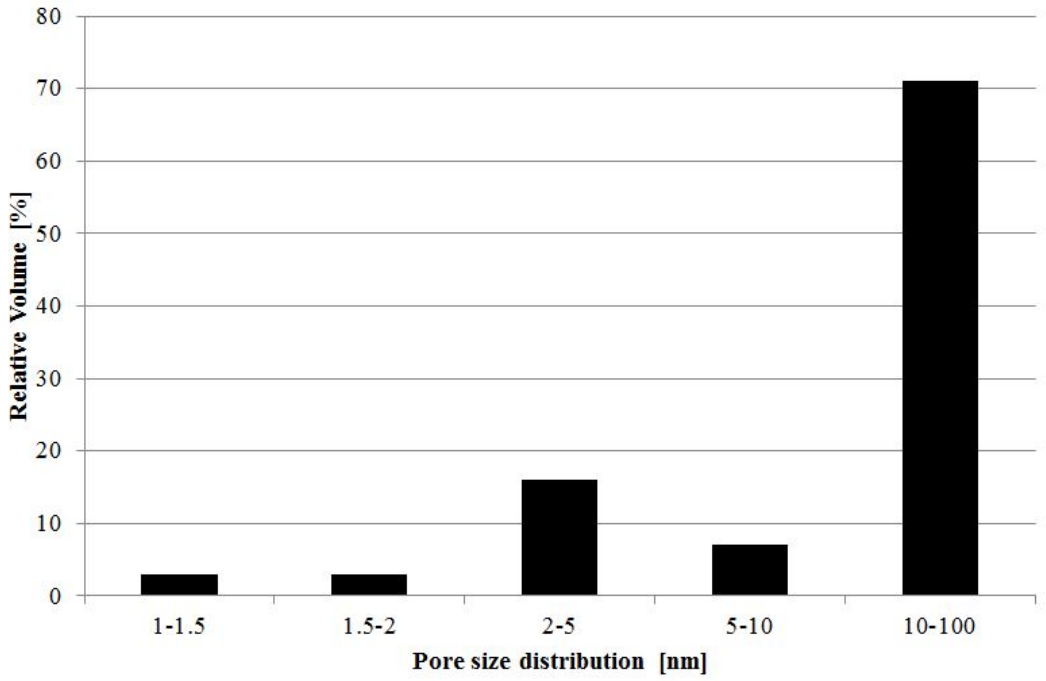

Figure 7.4: Pore size distribution of the raw algae material.

7.4.2 600 $°C$ and 2:1

This section describes the surface area and pore size distribution analysis for the activated carbon sample prepared at 600 $°C$ and with a KOH/algae raiot of 2:1. This sample was tested using a software setup for low porosity materials. It was expected that the sample had a high porosity but since time was a huge constraint the fastest program was chosen. Figure 7.5 shows the adsorption desorption isotherm of the activated carbon sample prepared at 600 $°C$ with an KOH/algae ratio of 2:1. The shape of the curve is s-shaped and of type IV with a hysteresis indicating mesoporosity.The hysteresis loop is of type H3 which indicated slit-shaped pores. The BET surface area was 92 $\frac{m^2}{g}$. This was a very small surface area compared to what was expected. Also it was too small. for it to be used as activated carbon. The C value was 176 which was a nice high value.

Figure 7.6 shows the pore size distribution of the activated carbon prepared at 600 $°C$ with an KOH/algae ratio of 2:1. The pore size distribution is identical to the one for the raw algae material. This means that either there was a failure in the program or the activation did not change the pore size distribution. The second option is highly unlikely since a previous study [9] showed that there were changes between activated carbons prepared at different temperatures. Also the isotherms have identical shapes and only the scale

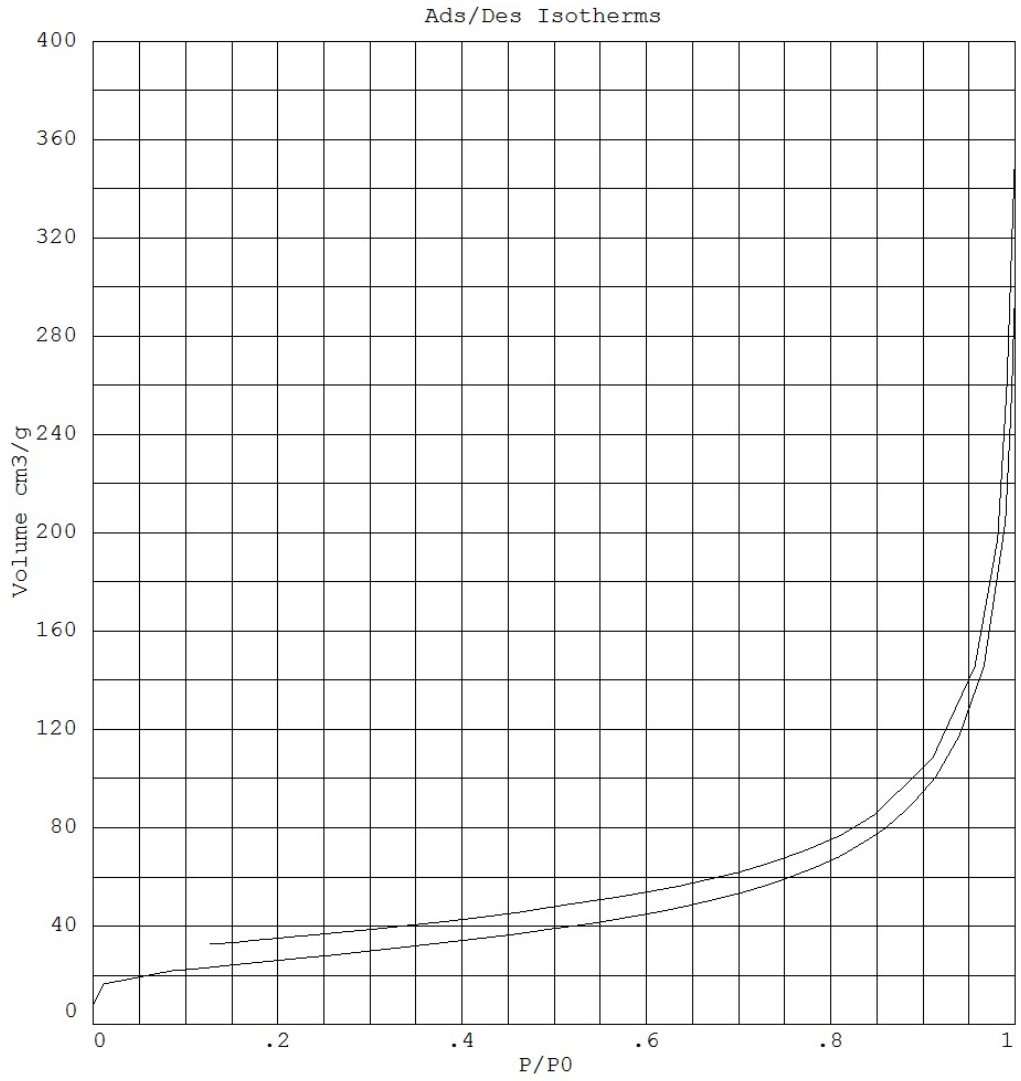

Figure 7.5: Adsorption-desorption isotherm of N_2 at -196 $°C$ on activated Fucus vesiculosus algae collected from Kolding prepared at 600 $°C$ with an KOH/algae ratio of 2:1.

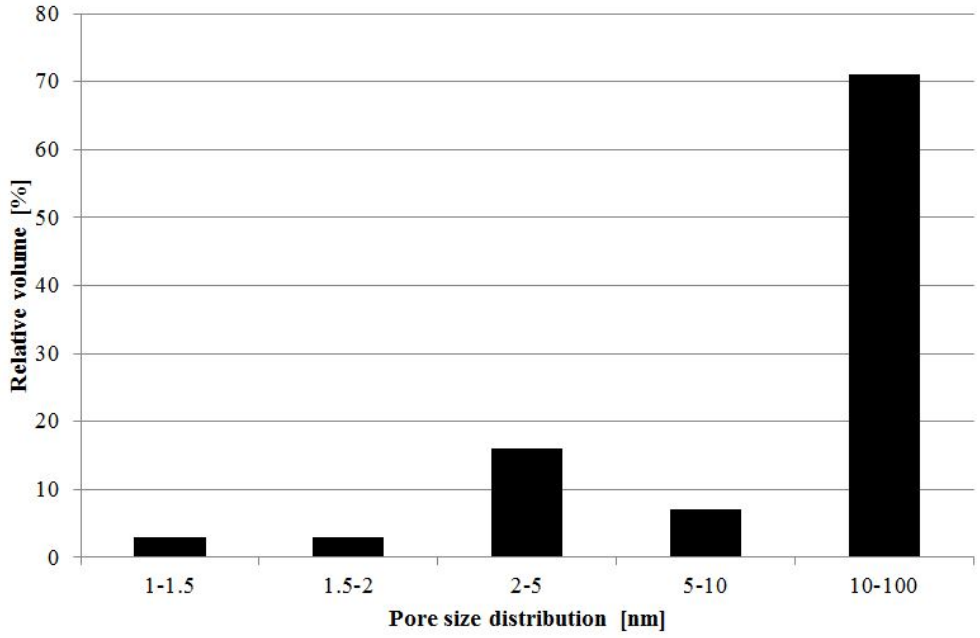

Figure 7.6: Pore size distribution of activated carbon prepared at 600 $°C$ with an KOH/algae ratio of 2:1.

of the vertical axe is different. This sample was tested with the same setup for the software as for the raw algae sample so perhaps the setup of the software created these similarities. This strange discovery led to another study of the H_2SO_4 activated sample tested using two different program setups.

7.4.3 H_2SO_4 Activated

This sample was tested using a software setup for high porosity materials. Figure 7.7 shows the adsorption ande desorption isotherm for the H_2SO_4 activated algae of the specie Fucus vesiculosus collected from a beach near Kolding. The shape of the isotherm is a combination of a type I and type IV isotherm since the initial slope is higher than the one for the raw algae material. However the plateau is not completely horizontal and some adsorption occur at high relative pressure. This shape indicated that the material had micropores as well as mesopores. Also there is a clear hysteresis loop similar to a type H4. This type of hysteresis loop indicates slit-shaped micropores. The BET surface area of this sample was 690 $\frac{m^2}{g}$ according to the instrument. The is a low surface area compared to the one shown in table 2.2 and in figure 3.9. Therefore this material might not be the best for adsorption. However the C

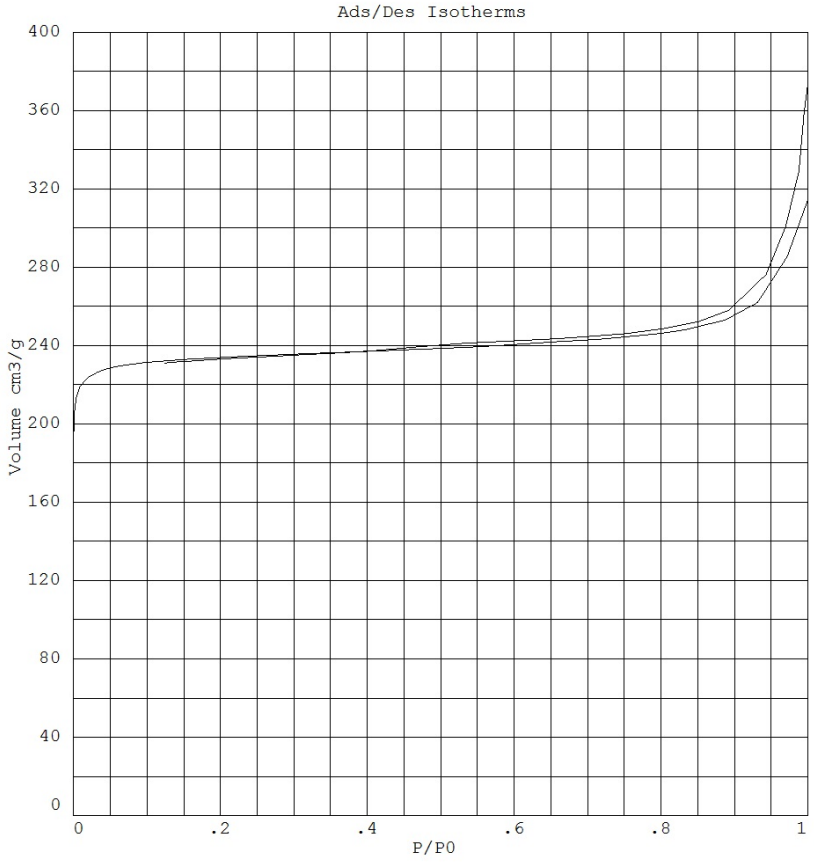

Figure 7.7: Adsorption-desorption isotherm of N_2 at -196 $°C$ on H_2SO_4 activated Fucus vesiculosus algae collected from Kolding.

value of this sample was -41. As described and shown in section 7.2 a negative C value has no physical meaning. A way to deal with a negative C is the narrow down the BET range. This was done by producing the BET plot from the adsorption data. The plot in shown in figure 7.8. The figure shows that the data points to the right caused the intercept of the line to be negative. By removing the data points one by one an positive C value could be obtained. At each step the new BET plot was made and the slope and intercept was registered. The procedure is shown in table 7.2. The table shows that six data point had to be removed in order to obtain a positive C value. The C value was calculated using equation 7.33, V_m was calculated using equation 7.32, and the specific surface area SA_{BET} was calculated using equation 7.40. The obtained C value after removal of six data points was extremely high. However, when more data points were removed the value of C slowly decreased but the influence on V_m and SA_{BET} were very small. Therefore no more points are given in the table. Notice that the BET surface area calculated using the plot and equation 7.40 did not at any time give the same as the instrument. This

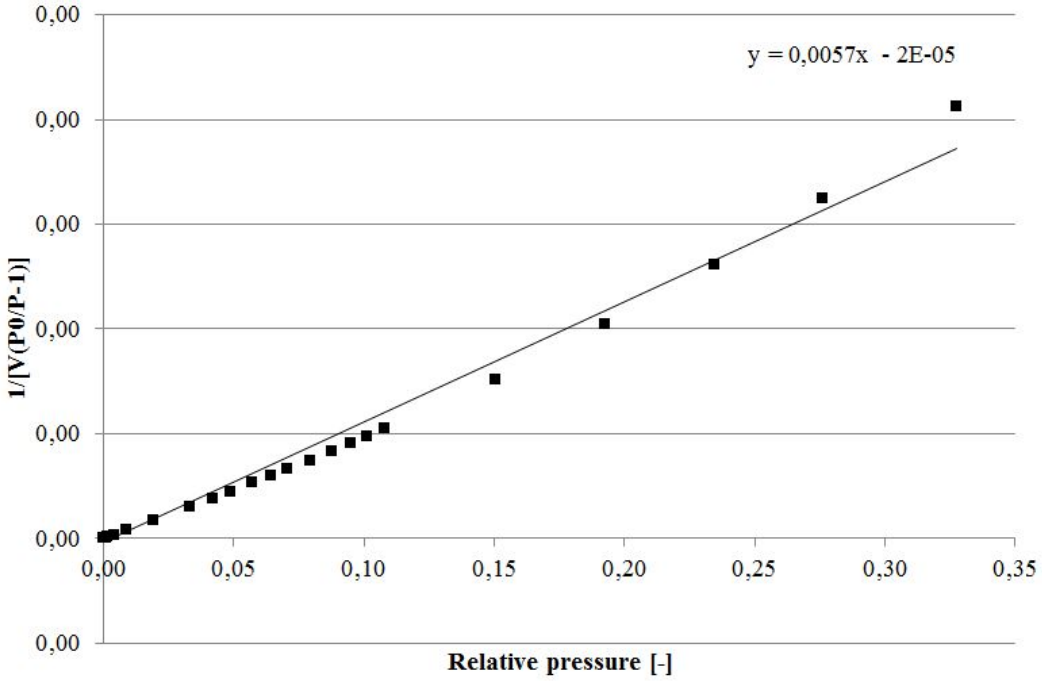

Figure 7.8: BET plot for the activated carbon sample prepared using H_2SO_4. The equation of a linear line through the data point is given. No data points are removed so far.

Table 7.2: Procedure to obtain a positive C value for of the H_2SO_4 activated carbon sample.

Data points removed from the right of the BET curve	Slope	Intercept	C $[-]$	V_m $\left[\frac{m^3}{g}\right]$	SA_{BET} $\left[\frac{m^2}{g}\right]$
0	0.0057	-2E-05	-284	176	767
1	0.0054	-1E-05	-539	186	808
2	0.0052	-6E-06	-866	193	838
3	0.0050	-3E-06	-1666	200	871
4	0.0048	-1E-06	-4799	208	907
5	0.0047	-1E-07	-46999	213	926
6	0.0047	1E-08	470001	213	926

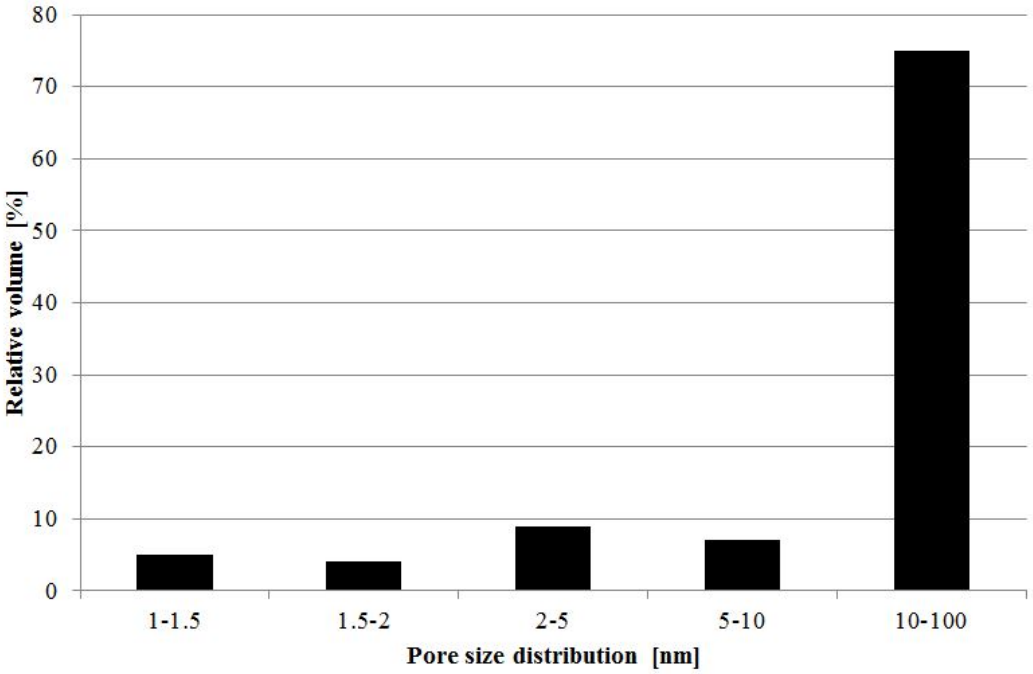

Figure 7.9: Pore size distribution of H_2SO_4 activated algae.

indicated that the calculation of the surface have been set up in a different manner than equation 7.40. They are on the other hand in the same range and can therefore still be used for comparison with other tests.

The pore size distribution of the sample is shown in figure 7.9. The distribution is very similar to that of the raw algae material shown in figure 7.4. This means that H_2SO_4 activation does not change the pore size distribution of the material. Instead it just increases the surface area. If mesopores were desired this would not have been a problem. In this project micropores are highly wanted and therefore is this material not optimal for adsorption of sour gases.

Some questions were raised concerning the two previous tests. Due to the similarity of the tests of the two previous samples it was intended to try to test the H_2SO_4 activated sample using the same software setup. The new adsorption-desorption isotherm is shown in figure 7.10. The BET surface area was given to be 46 $\frac{m^2}{g}$. This is a completely different number compared to the sample analysed with the high porosity program. A difference of hundreds of square metres per gram should not be possible. Also comparing the shape of the isotherm to the two other also produced using the low porosity program it is shown that they again are completely identical. This seems very strange and the results are therefore highly questionable. Due to this it was not found necessary to work any further with the results of this sample.

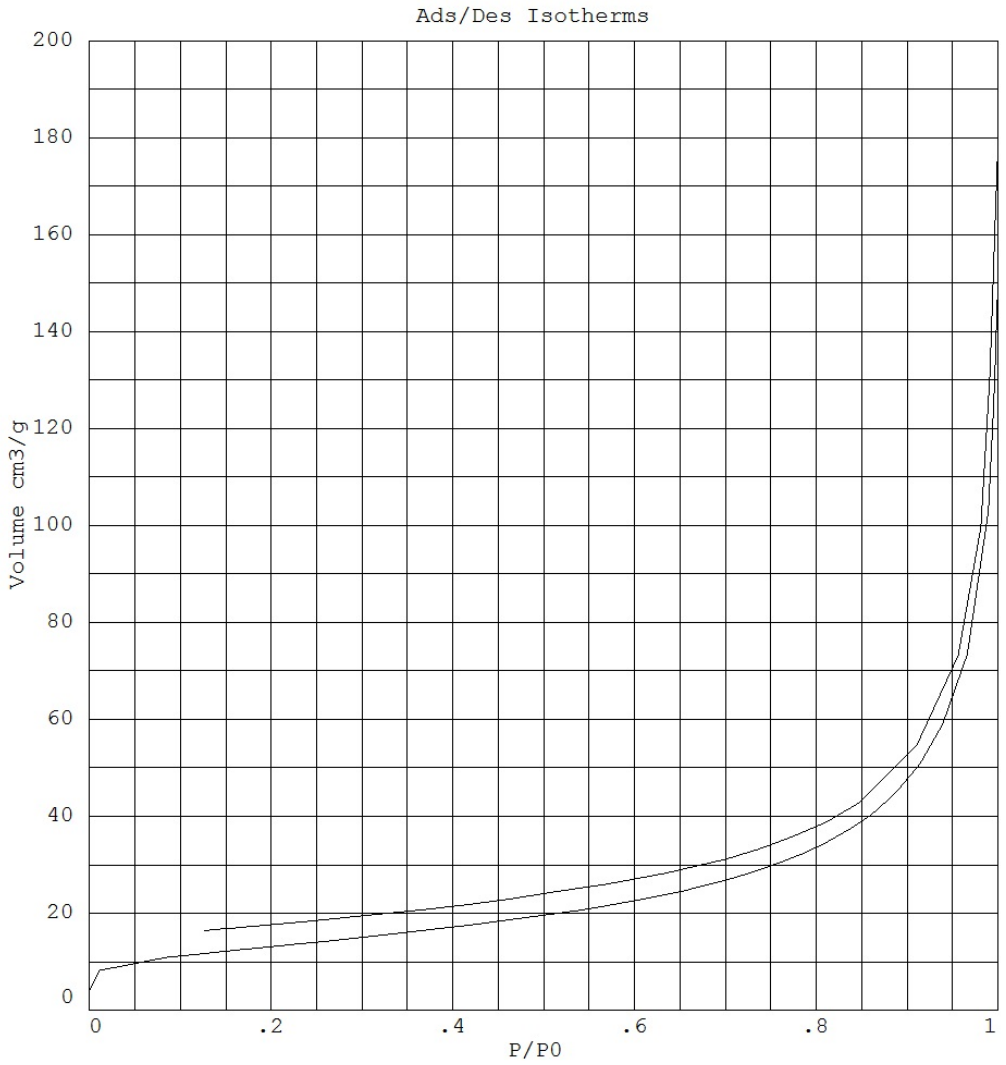

Figure 7.10: Adsorption-desorption isotherm of N_2 at -196 $°C$ on H_2SO_4 activated Fucus vesiculosus algae collected from Kolding. This curve was produced using the BET software low porosity program.

7.5 Evaluation

In appendix B the BET plots are given together with the calculated BET surface areas. These areas were almost identical to the ones calculated by the instrument which indicated that the theory and values described in this chapter is the same or similar to the ones used by the instrument.

The BET instrument gave an indication of the surface area of the samples. However the BET surface area must not be evaluated as the absolute surface area. However, it can be used to compare the samples with other activated carbons also measured using the BET theory.

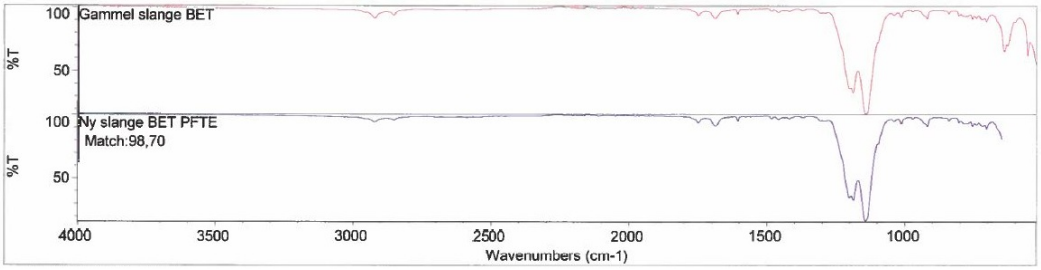

Figure 7.11: The IR spectra of the tubes used for the BET instrument. The top spectrum is for the old tube. The bottom spectrum is for the new tube.

The BET instrument had not been in use for many years when this project started and it was moved since the last time it was used. Therefore a lot of time during this project period was spent trying to understand the instrument and set it up. Even though the method is the same two different instruments for BET measurements might not work in the same manner. Because the BET instrument was moved to a new lab it had to be connected to gas lines once again. Some time was therefore spend trying to understand the purpose of the gas lines entering the instrument. It was discovered that the instrument used nitrogen gas as a carrier gas for the liquid nitrogen. Also the software of course demanded some attention. Unfortunately the tube connecting the dewar for liquid nitrogen with the small dewar used to cool the sample during tests broke during a refill of the second sample run. An investigation was initiated in order to find a material able to replace the tube. The plastic type PTFE, also known as Teflon, was chosen based on its good thermal resistance. The old tube and the new was investigated using FTIR. The results showed that the two tubes were exactly identical. The spectra of both tubes are shown in figure 7.11. The figure shows that the two spectra are almost identical which means that the old tube is most likely also a PTFE tube. Unfortunately some weeks went by before a new tube arrived in the beginning og June, which was the cause of more lost time. The yield after this episode was that the type of tube was now known and it could easily be replaced in case of another accident.

Another challenge was the duration of the analysis. The degas of a high porosity sample was around five hours. Then producing the adsorption-desorption isotherm could take between five hours and several day, depending on the size of the surface area and the program setup. This was a challenges as the dewar for the liquid nitrogen had to be refilled. It was expected that the nitrogen had to be refilled every seventh hour, but since the temperature was high during the period of the experiments the duration had to be reduced to every fifth

hour. After some refills it was apparent that at night the liquid nitrogen lasted a bit longer than in the day time due to lower temperatures. The BET instrument was located at the fourth floor in a relatively warm laboratory. Some liquid nitrogen could be saved by moving the instrument to a colder location. In order to minimise the heat in the daytime the curtains in the room were closed which created a significant temperature decrease during the daytime.

Strange results came out of the two tests using the H_2SO_4 activated carbon. One measurement using the high porosity setup of the software showed a surface area of approximately 900 $\frac{m^2}{g}$ where a low porosity setup of the software gave a surface area of approximately 40 $\frac{m^2}{g}$. This difference is too significant to be accepted. I seems like that when the type of program is chosen the range of the surface area and the shape of the isotherm are already defined by the software. This should not be the case but all the tests points towards that. The three samples prepared using the same software setup produced the exact same shape of the isotherms. Also the pore size distributions are to similar to seem correct. Some deviation must be expected, however that is not shown from the results. The software setup for low porosity and high porosity is simply a matter of the amount of adsorption points and the allowed equilibrium deviation. Therefore huge differences in the outcome should not happen. The best way to secure the validity of this BET instrument would be to test the same samples using another BET instrument.

Adding all the challenges together made it hard to perform all the wanted tests. The tests with the cultivated microalgae, the activated algae prepared at different KOH/algae ratio as well as a test using the algae collected near Esbjerg had to be postponed. This was naturally very unfortunate, however the main focus of this project was the usage of the Danish macroalgae and therefore it had a higher priority. The algae collected at a beach near Esbjerg had a lower priority since the type of algae was unknown and the amount collected was small. Of course the main goal of this project was to prepare all the algae in the same manner and perform the same tests with them to find the better one. Unfortunately, that was not possible due to all the challenges encountered during the entire project period. This opens up for the possibility to perform many more tests with new and repeated samples. The tests of the same samples should be repeated to tests the validity as well as new samples should be prepared in order to test the reproductive performance. The conclusion to this was that the experiments in this chapter gave a good indication of that Danish macroalgae can be used for deriving activated carbon materials with an increased surface area compared to the original algae material.

CHAPTER 8

Test of Adosorption of Sour Gases

Just determining the surface area of the activated carbon is not enough to decide if the material is useful for adsorption of sour gases. In section 1.4 an alternative method to remove sour gases from natural gas was proposed. The idea was to inject the gas into a flask containing the activated carbon sample which then could adsorb the gas. Common for the tests of adsorption of H_2S and CO_2 were that they were tested in a non-closed system meaning that before, during and after adsorption tests the samples were exposed to air. This way it was possible to see if any of the sour gases adsorbed onto the activated stayed there after exposure to air. It is highly unwanted to have an adsorption system were the adsorbate desorbs from the adsorption material when exposed to air since that would make the handling of the system much more complicated.

The samples used for these tests were activated prepared by conventional chemical activation and H_2SO_4 activation at Aalborg University Esbjerg. Also the raw algae material as well as a commercial available activated carbon were tested for comparison.

8.1 Test of H_2S Adsorption

The adsorption of H_2S was tested using the test setup shown in figure 8.1. The flask to the left contained iron sulphide (FeS). Slowly concentrated hydrochloric acid (HCl) was added to the flask in order to produce H_2S according to the reaction:

$$FeS + HCl \rightarrow FeCl_2 + H_2S \tag{8.1}$$

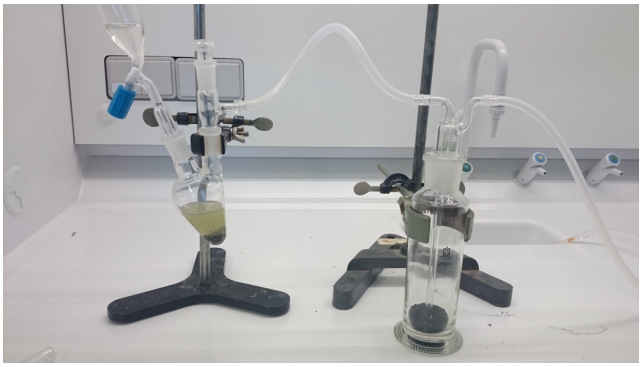

Figure 8.1: Test setup for adsorbing H_2S onto activated carbon.

Figure 8.2: The elemental analysis test setup.

The H_2S was then led to the flask to the right containing the activated carbon sample. The idea was to have the activated carbon adsorb the produced H_2S in order to test its ability to adsorb sour gases. Naturally all tests were performed in the fume hood. The activated carbons were compared to the commercially available activated carbon Chemviron Carbon. The tests were performed in 1-3 hours.

In order to determine if H_2S did adsorb onto the activated carbon materials the composition of the material before and after exposure to H_2S should be compared. For this elemental analysis was used. The test setup is shown in figure 8.2. To the right a scale is placed. The scale was used to measure the mass of the sample. The sample was wrapped in aluminium and placed in one of the holders on the top of the instrument to the left. Here the samples were injected one after the other for analysis. Details about the method of elemental analysis can be found in appendix C.

The analysis were performed using activated carbon before and after exposure to H_2S. Besides the use to compare if the adsorption of H_2S was successful the

analysis were also used to compare the composition of the different carbons. Specially the difference between the algae found at the beach near Kolding, Fucus vesiculosus, and the algae found at the beach near Esbjerg. Every sample was analysed at least three times in order to secure that the results are representative.

8.1.1 Results

The comparison between the two algae types is shown in table 2.1.

The main results are shown in table 8.1. The weight was the chosen mass of the sample which should be between 1 and 5 mg. The most interesting part of the table is the percentage of sulphur. The idea was to see an increase in content of sulphur when a sample had been exposed to H_2S. Looking at just the dried raw algae a small increase in sulphur content can be observed. That means that the material naturally was predisposed to adsorb H_2S. However, this could of course be destroyed by the activation procedure. The same tests were repeated for different activated carbon samples. For each sample a least three runs were performed in order to secure validity of the results.

Coming then to the H_2SO_4 activated carbon the natural content of sulphur was relatively high. The reason for this could be the activation process using H_2SO_4 increased the sulphur content. Some sulphur must have reacted or attached itself to the algae and thereby increased the total sulphur content. After exposure to H_2S only a very small increase in the sulphur content could be observed. This could be an indication for that the H_2SO_4 activated carbon was not suitable for H_2S adsorption.

The next activated carbon was the one prepared at 600 $°C$ and with a KOH/algae ratio of 2:1. The sulphur content of that material was very small. This means sulphur was removed from the algae during activation. However after exposure to H_2S the amount of sulphur increased significantly. These results indicated that activated carbon prepared at this temperature with this KOH/algae ratio was very suitable for H_2S adsorption. However these results must be compared with the measurements of surface area in order to determine the total adsorption capacity.

Adsorption experiments were not performed with the activated carbon prepared at 700 $°C$ and with a KOH/algae ratio of 2:1 due to the time restraints. However, elemental analysis was performed in order to observe the changes between the different activated carbons and compare them with the original

algae material. The sulphur content was the same as for the activated carbon prepared at 600 $°C$ and with a KOH/algae ratio of 2:1.

Finally the sulphur content of the activated carbon prepared at 800 $°C$ and with a KOH/algae ratio of 2:1 was found to have the same sulphur content as the ones prepared at lower temperature. However the carbon content decreased significantly. Also the nitrogen content decreased. Moving to the adsorption test with that material it is shown that the sulphur content increased. However, not as much as for the sample prepared at 600 $°C$ and with a KOH/algae ratio of 2:1. This indicated that a higher temperature might decrease the adsorption properties for H_2S adsorption. The carbon content of this sample was very low. An explanation for this could be that the furnace was not completely air tight and some air might have entered the furnace during activation. Since to plugs used to tighten the furnace were new and untested the knowledge about them and their ability to keep the furnace airtight was uncertain. A leak could explain an increased oxygen content which would result in a decreased percentage of carbon.

Comparing to the adsorption of H_2S for the commercial Chemviron activated carbon the adsorption of the algae derived activated carbon seemed to be a much better option.

The reason for the decreased adsorption capacity for H_2S of the sample prepared at 800 $°C$ and with a KOH/algae ratio of 2:1 compared to the sample prepared at 600 $°C$ and with a KOH/algae ratio of 2:1 could be found in the nitrogen content. If the nitrogen in the material is bound in an alkaline group such as an amine, sour gases such as H_2S would be more inclined to adsorb on the material.

General for all the tests is that when the sulphur content goes up the carbon content goes down.

Table 8.1: Results of the elemental analysis. The samples are raw algae, H_2SO_4 activated carbon, activated carbon prepared at 600, 700 and 800 $°C$ and commercial activated carbon Chemviron. For all except one sample adsorption of H_2S was tested. Notice that the oxygen content is not given by the EA instrument, it should be considered to represent the remaining percentage.

Sample	**Weight**	**Percentage**			
	$[mg]$	**Carbon**	**Hydrogen**	**Nitrogen**	**Sulfur**
Algae	6.06	40.4	4.44	2.66	1.85
	4.488	40.08	5.33	2.44	1.99
	4.91	37.25	5	2.35	1.79
Algae + H_2S	2.145	40.12	5.76	2.51	3.52
	4.048	39.95	5.21	2.83	2.23
	3.682	39.85	5.48	2.62	2.33
H_2SO_4 activated algae	1.755	50.3	1.37	6.46	5.64
	1.161	50.28	1.18	5.96	4.2
	6.442	51	2.13	6.08	5.48
H_2SO_4 activated algae + H_2S	1.645	43.15	1.59	4.42	6.49
	4.798	35.03	1.69	4.37	8.67
	4.675	37.38	1.78	5.65	7.72
600 $°C$ 2:1 activated	1.196	29.72	0.47	0.89	0.7
	1.85	27.95	0.98	2.16	1.7
	1.217	29.23	0.65	3.43	0.63
600 $°C$ 2:1 activated + H_2S	1.337	17.54	0.33	0.44	28.28
	1.884	17.85	0.44	0.51	20.16
	2.095	21.21	0.94	1.01	25.24
700 $°C$ 2:1 activated	1.041	35.43	1.22	2.22	1.55
	1.848	34.7	1.33	1.82	0.93
	1.559	35.19	1.28	2.18	0.66
800 $°C$ 2:1 activated	2.31	13.33	0.92	0.28	0.82
	3.523	13.36	1.14	0.26	0.29
	3.46	13.29	1.22	0.3	0.31
800 $°C$ 2:1 activated + H_2S	2.327	13	0.61	0.18	1.96
	2.506	12.82	0.71	0.2	1.95
	3.672	12.84	1.01	0.19	1.94
Chemviron	6.501	77.02	0.33	1	0.01
	2.324	65.27	0.16	0.58	0.03
	3.121	77.27	0.18	0.85	-0.01
Chemviron + H_2S	2.729	80.78	0.3	0.56	0.26
	3.346	78.45	0.31	0.67	0.59
	2.723	75.29	0.44	0.53	0.65

8.2 Test of CO_2 Adsorption

The adsorption of CO_2 was tested using the extractor shown in figure 8.3. The vial containing the sample was placed at the right side of the extractor were the outlet was located. Here the vial was attached to the outlet and while running the extractor, CO_2 was blown into the vial. The gassing was performed for 3 minutes. This would make it possible for the sample to adsorb some of that CO_2. The idea was that using Fourier transform infrared (FTIR) spectroscopy an increase of CO_2 could be detected by observing the size of the peak at a wavenumeber of approximately 2300 cm^{-1}. The details of the method is

Figure 8.3: Extractor used for CO_2 adsorption experiments.

described in appendix D. It was assumed that the sample after exposure to air was saturated with CO_2. However it was also expected that the activated carbon samples were able to adsorb more than what the CO_2 in the air could provide. The IR spectrum was measured before and after exposure.

8.2.1 Results

Figure 8.4 shows the IR spectrum of the activated carbon sample prepared at 600 $°C$ and with a KOH/algae ratio of 2:1 before (red) and after (green) exposure to CO_2. This sample was chosen do to its good adsorption properties towards H_2S. There was a very small peak around 2300 cm^{-1}. Unfortunately the peak of the curve before and after gassing with CO_2 are identical. This indicated that the material might already have been saturated with CO_2 and was not able to adsorb more. It was expected that due to the local dipole

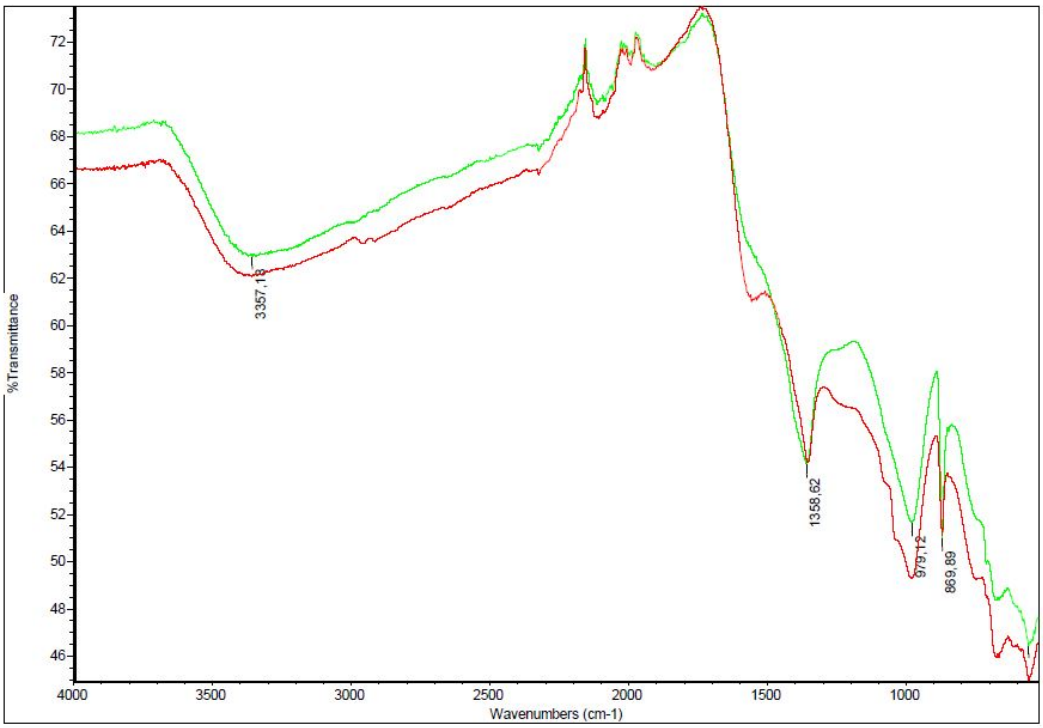

Figure 8.4: IR spectrum for the activated carbon sample prepared at 600 $°C$ and with a KOH/algae ratio of 2:1 before (red) and after (green) exposure to CO_2.

of CO_2 it would be able to perform physical adsorption on the surface of the activated carbon. However from the results this seemed not to be the case and more tests should be performed in order to discover the reason for this.

8.3 Evaluation

In section 8.1 the results indicated that algae derived activated carbons can be used for H_2S adsorption. From this study it seemed like the sample prepared at 600 $°C$ and with a KOH/algae ratio of 2:1 was the better choice. However more tests similar produced materials should be performed in order to validate the results.

The test with CO_2 adsorption in section 8.2 was on the other hand not as successful. It was not possible to show an increase in CO_2 content after exposure to larger amounts. There can be more explanations for that. Either the experimental method was not good enough or there will never be any further adsorption of CO_2. A way to test if the method is applicable is to degas the sample and then place it at the FTIR to measure the adsorption of CO_2. This

could show if the adsorption process is measurable.

The duration of each H_2S adsorption test was between one hour and three hours depending on how much the valve was opened. All samples had to be collected before elemental analysis could be performed. The duration of each test in the elemental analyser was eight minutes. In order to secure homogeneity of the results each samples was tested at least three times. Producing the adsorption samples required some days while the analysis in required a couple of hours. The only way to optimise the duration of this experiment was to optimise the mixing of the acid and the iron sulphide. However, the acid must not be added to fast since too high concentrations of H_2S would be produced.

The duration of a CO_2 adsorption experiment was thirty minutes. As no change in CO_2 content of the sample was detected the duration of this experiment should not be reduced. By increasing the duration it might be possible to measure a difference in concentration. The analysis by the FTIR spectrometer demanded only a few minutes and could therefor not be further optimised. Since specially the activated carbon prepared using H_2SO_4 was very brittle it was difficult to fasten the material in the FTIR spectrometer. The samples prepared using pyrolysis were much more suited as the had a more soft texture.

CHAPTER 9

Discussion

One of the main challenges using activated carbon filters are the logistics. How to clean it, should it been done on site or should it be moved to a cleaning facility? Onshore the problems are not so dominating since there is less space restrictions and transportation of the material is easier. However, offshore it is much more problematic to handle solids. It is highly unwanted to ship solids back and forth therefore, if an activated carbon filter is to be used offshore, a better solution must be found. A suggestion is to perform the cleaning of the activated carbon filter on site. This means that for example using a washing step the H_2S and CO_2 adsorbed onto the activated carbon can be transferred into the water due to their good solubility in water. This way the transportation away from the installation should be more convenient. This can only be done due to the unlimited access to sea water at offshore installations.

Analysing the activation technique the usage of chemicals for activation could be a problem due to the cost. Also the fact that in water the prepared samples are highly alkaline could be a safety issue. This demands extra precautions of the handling of the samples during different operational procedure such as washing. Therefore the amount of chemical used compared to the extra gain of surface area must be considered carefully. Also, the activation temperature must be taken into consideration. A higher temperature means a higher cost. Therefore the extra gain in surface area must be compared to the cost of using a higher temperature. Not always is it profitable to produce the most effective material. If the gain from using more chemical or higher temperature is only a few percent, then it might not be the best solution economically.

Really interesting results were featured in section 8.1. The results indicated that the algae derived activated carbon prepared at 600 $^{\circ}C$ was by far the

most effective for H_2S adsorption. However, in order to be able to conclude anything more identical test should be performed. If an identical experiment shows the same results the material could be a very strong candidate for an activated carbon material for removal of H_2S.

There were several obstacles during this project period. Unfortunately some of the equipment had not been used to for many years and therefore had to be set up again. Also the need to order spare parts was a challenge as it was not in stock and had to be fabricated before shipment. Plugs for the furnace was ordered in the beginning of the project period but first arrived in the end of May. Just before that the tube used to transport liquid nitrogen for the BET instrument broke. The new tube arrived in the beginning of June. All these challenges in the end caused many delays in the time schedule. If it was not for these delays more test with different activated carbon could have been performed according to the original plan. This was a highly unfortunate situation as many tests were planned which altogether could have provided at good idea of how the different activation parameters would have affected the final product. However a previous study [9] gave an indication of how KOH/algae ratio and activation temperature affected the activated carbon products. Based on the results from that study it would have been natural to prioritise that samples prepared at 900 $^{\circ}C$ and with a KOH/algae ratio of 2:1. However, due to the interesting results in section 8.1 concerning the adsorption of H_2S it was chosen to move the focus to the samples prepared at lower temperatures.

CHAPTER 10

Conclusion

In the present work many aspects concerning activated carbon were addressed. Experiments demonstrated two methods of chemical activation of algae derived activated carbons. A pyrolysis process using KOH as activating agent created a slight increase in surface area but gave good adsorption properties. Specially the sample prepared at 600 $^{\circ}C$ and with a KOH/algae ratio of 2:1 showed really good adsorption properties towards H_2S. A sample prepared using H_2SO_2 showed the highest surface area, however the adsorption capacity towards H_2S was to weak. For the analysis of the adsorption capacity of H_2S, elemental analysis were performed. Also the adsorption capacity of CO_2 was tested using the sample prepared at 600 $^{\circ}C$ and with a KOH/algae ratio of 2:1. The capacity was tested using FTIR. Unfortunately no increase in CO_2 content could be detected after exposure.

The pyrolysis process was investigated using thermogravemetric analysis. The analysis showed that by adding KOH to raw dried algae, the burn-off was reduced meaning that approximately 70% of the original mass was preserved. Comparing with a similar test with raw dried algae only 10% of the original mass was preserved after heating to 900 $^{\circ}C$. The reason for this was investigated by repeating these two test using pure cellulose. The results showed the exact same tendency as for the algae material. The theory is that in the beginning of the pyrolysis end group are removed from the material. At a certain temperature the end groups change instead of being removed to a much stronger composition.

The BET instrument was the main analysis method of this project. However, it might not have been the best method to test these samples. The BET instrument used produced some very strange result were as an example two software setups produced completely different results for the same sample. Also it seemed like that when a software setup was chosen the machine already

had an idea about the range of the surface area which could make it show a higher or lower result than what was really the case. Also the isotherms produced were identical for three samples, the only deviation was the scale on the vertical axe. The instrument should produce the isotherm from scratch instead of just plotting a template. All these issues combined caused great distrust of the instrument and its results.

The combination of the different challenges in this project resulted in that the preparation of the samples first could start in the end of May and the analysis could start in the beginning of June. Due to this samples were send to associate professor Vittorio Boffa at Aalborg University for him to prepare. Also it was tried to find an external BET instrument to use. Unfortunately without success. The outcome of this is that much more work can be done in the future within this subject. The results obtained and described in this project are promising but more work must be put into it before any final conclusions cam be made.

CHAPTER 11

Prospects

The many challenges of this project opened up for the possibility to make more samples and perform many more tests. Prospects for further work are:

- Test the selectivity.
- Optimise more on the activation method.
- Try alternative activation methods such as microwave heating.
- Test other activating agents.
- Test different doping techniques.
- Analyse the surface chemistry of different activated carbon to investigate why there are differences in the adsorption properties.
- Try to degas the samples before performing adsorption test to test the maximum adsorption capacity.
- Try to find the connection between equation 7.36 and equation 7.37.
- Test similar samples using another BET instrument to check the validity of the results in this project.
- Figure out the connection between KOH and the preservation of mass during pyrolysis.

APPENDIX A

Cultivation of Microalgae Scenedesmus

This appendix describes the process of cultivating the microalgae Scenedesmus in two different media: MWC/MWC-Se medium and universal fertiliser as shown in the figure A.1 and A.2.

A.1 Cultivation

This section describes the cultivation of the Scenedesmus in the two different media. The 9th of March 2016 it was placed inside the media. 400 mL of the original solution containing the algae was added to 1 L of MWC/MWC-Se medium and 500 mL of the algae solution was added to 1 L of diluted universal fertiliser.

The following figures contain photos of the two solution over time. The caption of each figure is the date the photo was taken in the format DD-MM-YY.

Figure A.1: Universal fertiliser from the front.

Figure A.2: Universal fertiliser from the back.

Figure A.3: 09-03-16.

Figure A.4: 16-03-16. Before adding more medium.

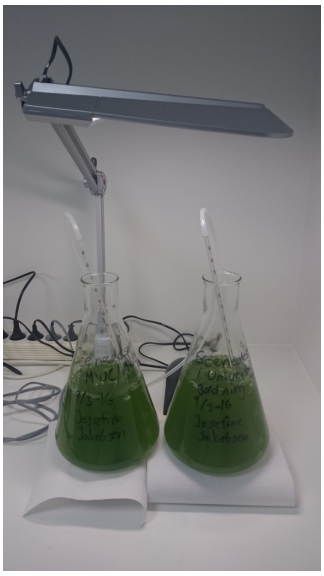

Figure A.5: 16-03-16. After adding 0.5 L of medium, MWC/MWC+Se and universal fertiliser to each respectively.

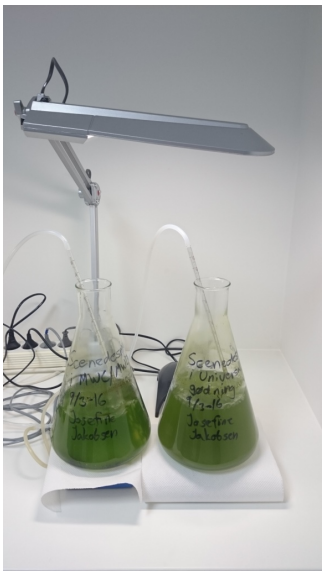

Figure A.6: 30-03-16. Before adding more medium.

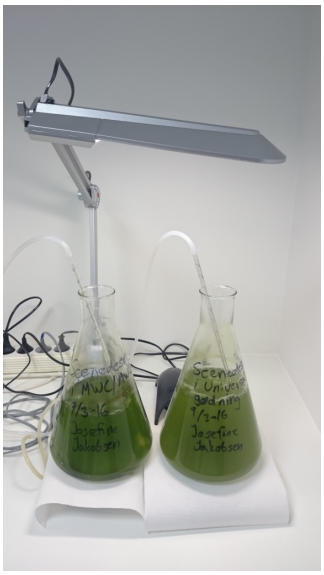

Figure A.7: 30-03-16. After adding 0.25 L of medium, MWC/MWC+Se and universal fertiliser to each respectively.

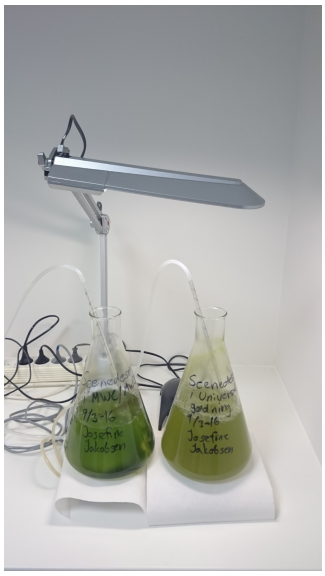

Figure A.8: 06-04-16. Before adding more medium.

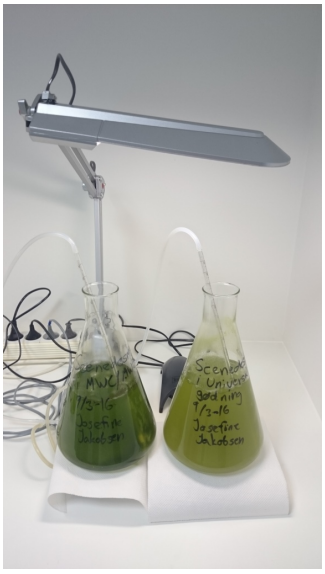

Figure A.9: 06-04-16. After adding 0.25 L of medium, MWC/MWC+Se and universal fertiliser to each respectively.

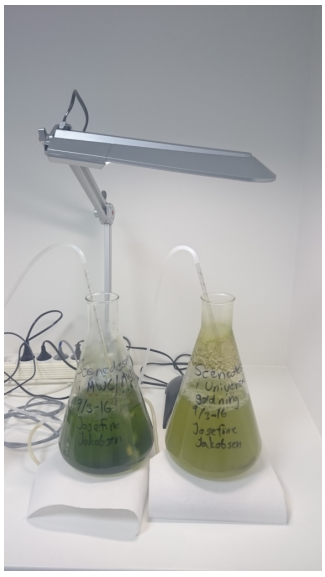

Figure A.10: 27-04-16. Before adding more medium.

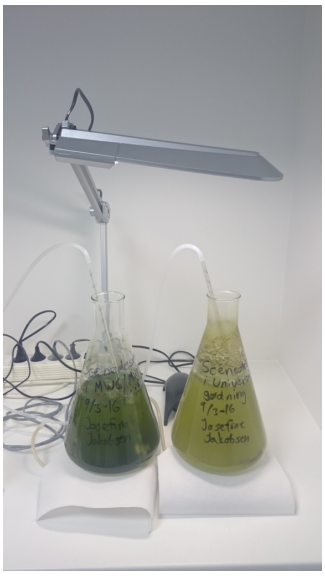

Figure A.11: 27-04-16. After adding 0.25 L of medium, MWC/MWC+Se and universal fertiliser to each respectively.

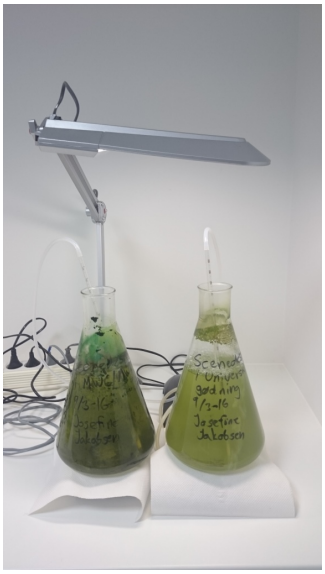

Figure A.12: 25-05-16. Before adding more medium.

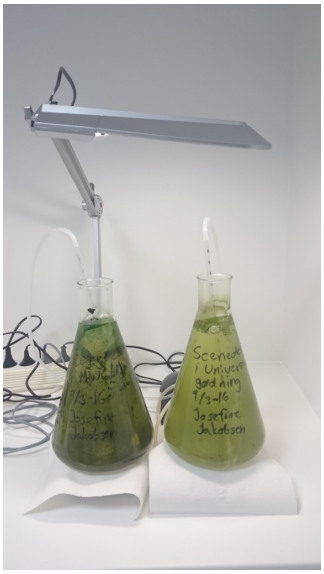

Figure A.13: 25-05-16. After adding 0.25 L of medium, MWC/MWC+Se and universal fertiliser to each respectively.

APPENDIX B

BET Plots

This appendix contain the linear BET plots of the experiments. An exception is the plot for the H_2SO_4 activated sample since that one is already presented in section 7.4.3. For the samples the BET plot is shown and used to calculate the BET surface area using the three equation 7.32, 7.33, and 7.40. In the figure text the calculated BET surface area is given.

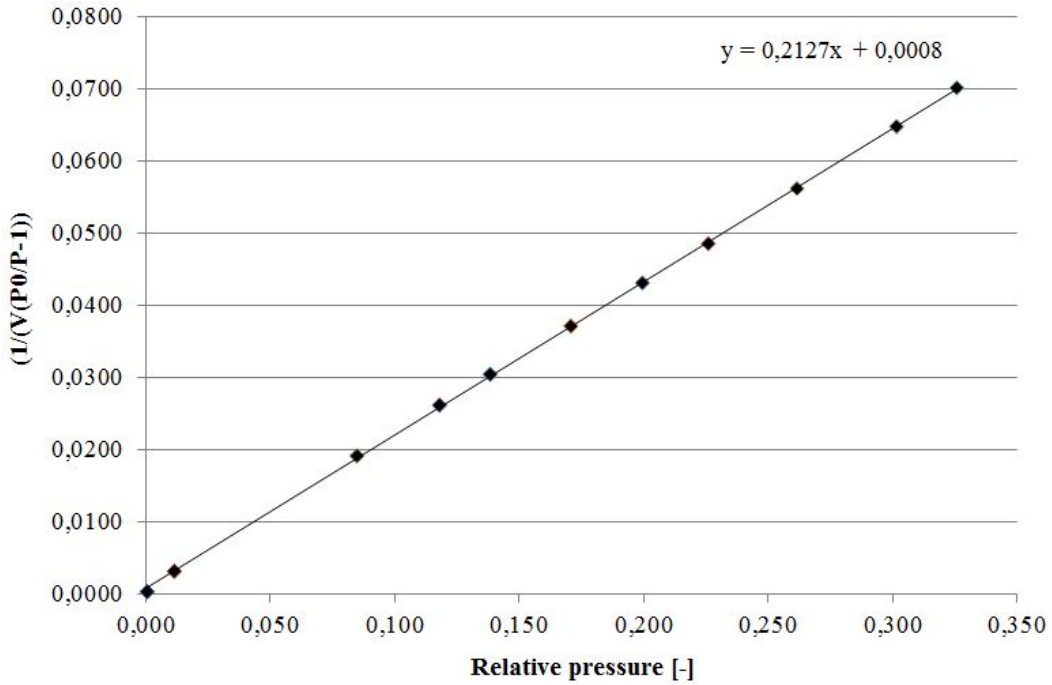

Figure B.1: BET plot for the raw algae material. The equation used to calculate V_m and C is given. The calculated BET surface area was 20.4 $\frac{m^2}{g}$.

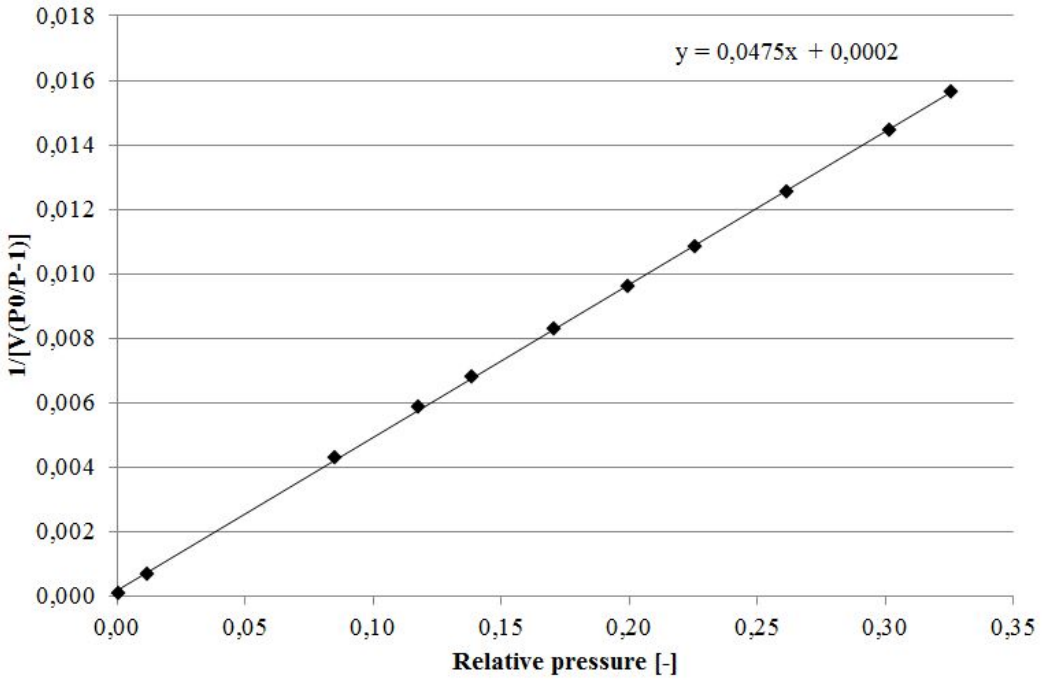

Figure B.2: BET plot for the activated carbon prepared at 600 $°C$ with a KOH/algae ratio of 2:1. The equation used to calculate V_m and C is given. The calculated BET surface area was 91.2 $\frac{m^2}{g}$.

APPENDIX C

Elemental Analysis

In elemental analysis compounds are oxidised to N_2 used to identify the nitrogen content, CO_2 used to identify the carbon content, H_2O (saturated steam) used to identify the hydrogen content, and sulphur dioxide (SO_2) used to identify the sulphur content. The residual percent is oxygen which is not directly measured by this method. Figure C.1 shows the principle of elemental analysis. Starting to the left, here are the gases used for the different steps of the processes stored. The next part is the combustion zone in which the sample is burned with an excess of oxygen. Here the sample is combusted through a flash combustion causing immediate oxidation of the sample [41, 40]. Hereafter is the gas control zone. The gases produced in the combustion zone are captured and mixed. Helium was used as a carrier gas. In the chamber pressure, temperature and volume are controlled. When a homogeneous mixture is achieved the chamber was depressurised. The gases are then led through the separation zone using the technique frontal chromatography [40]. Basically frontal chromatography is a chromatographic separation process where the sample is injected into a chromatographic bed continuously. The components then

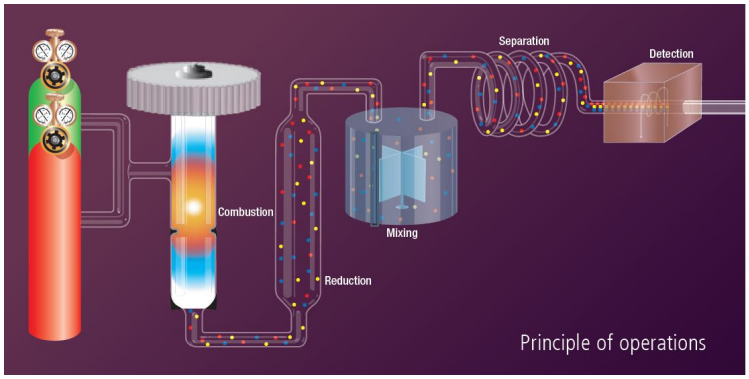

Figure C.1: Principle of CHNS elemental analysis. [40]

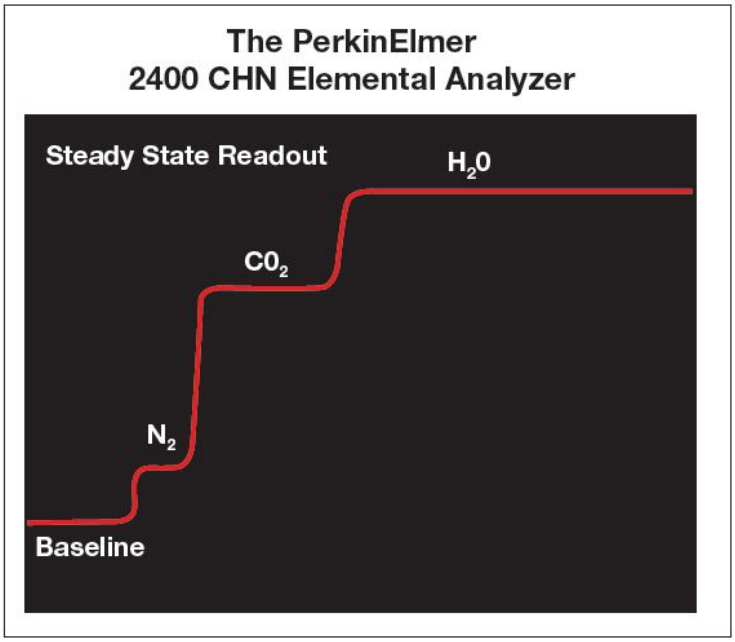

Figure C.2: Chromatogram showing the principle of the separation process as well as the detected components. [40]

Table C.1: Thermal conductivities of gases detected in elemental analysis at 25 $°C$. [43]

Gas	Thermal conductivity at 25 $°C$ $\left[\frac{W}{m \cdot K}\right]$
N_2	0.024
CO_2	0.0146
H_2O	0.0184
SO_2	0.0086
He	0.142

emerge at different speeds and thereby separates. The order of which the components emerge are shown in figure C.2. The gases are then measured using a thermal conductivity detector. Often the thermal conductivity is much less for most compounds compared to helium and they will therefore be detected as a drop in conductivity [42]. Table C.1 shows the thermal conductivity of N_2, CO_2, saturated steam (H_2O), SO_2, and helium (He) at 25 $°C$. It is shown that He has the highest thermal conductivity and that there is a significant difference between the three others. Therefore the four gases can be detected in the thermal conductivity detector.

APPENDIX D

Infrared Spectroscopy

IR spectroscopy utilises the fact that molecules absorb specific frequencies based on their structure [44]. Different frequencies will have a different effect on the vibrations of the molecule. When the emitted IR frequency is the same of the vibrational frequency of a bond, absorptions occurs. In order for a molecule to be infrared active it needs to have a dipole moment changing during vibration [6]. The vibrational modes of a molecule can be divided into two groups; stretching and bending. The stretching vibration demands most energy and will therefore in the vibrational spectrum stretching vibrations will be found at higher wavenumbers [6]. However symmetrical stretching is not visible on an IR spectrum since the symmetrical movement does not create a changing dipole moment. The different vibrational modes are shown in figure D.1. CO_2 has four vibrational modes;

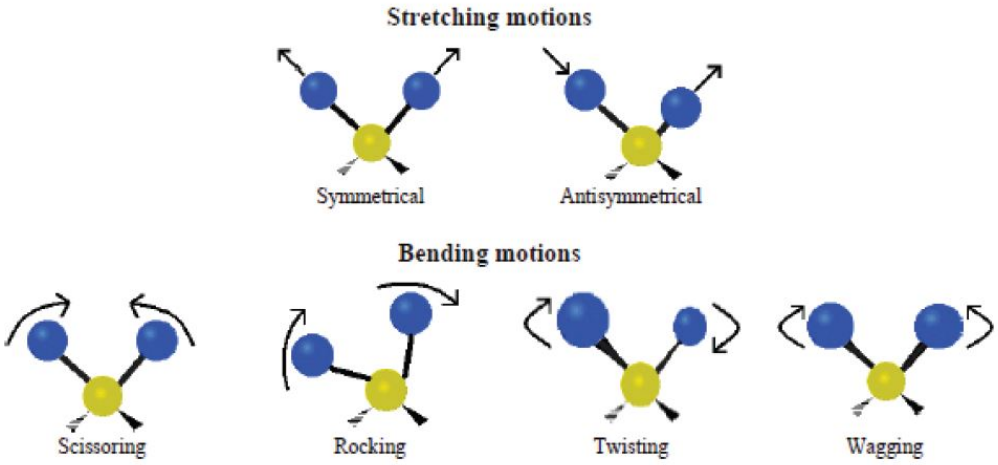

Figure D.1: Vibrational modes of molecules. [6]

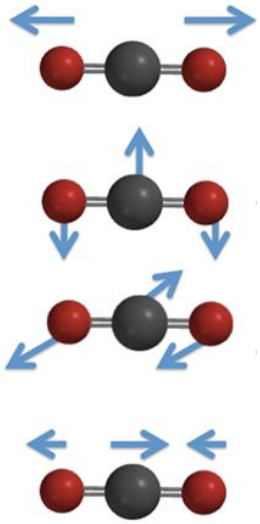

Figure D.2: Vibrational modes of CO2. [45]

- symmetric stretch,
- asymmetric stretch, and
- two bend modes, scissoring and wagging.

These modes are also shown in figure D.2. In this project Fourier transform ifrared spectroscopy (FTIR) was used. The main difference between the two methods is that normal IR sends the infrared beams directly through the samples to the detector. In FTIR mirrors first direct the light towards a diamond on which the sample is placed. Hereafter the light is reflected towards the detector to measure the transmittance.

Bibliography

[1] Josefine Rønn Jakobsen, Nikolaos Montesantos, and Ricardo Nuno Cardoso Machado Macedo. Fate of production chemicals in the off-shore sector. Master's thesis, Aalborg University, 2015.

[2] Tabita Lindeborg Hylkjær, 2015. Maersk Oil, Personal contact.

[3] James G. Speight. *The Chemistry and Technology of Petroleum*. CRC Press, fifth edition, 2014.

[4] Matthew R. Simmons. Oil and gas rust: An evil worse than depletion, 2008.

[5] Malcolm A. Kelland. *Production Chemicals for the Oil and Gas Industry*. CRC Press, second edition, 2014.

[6] Henrik Tækker Madsen. Investigation of fouling formation during h2s scavenging with 1,3,5-tri-(2-hydroxyethyl)-hexahydro-s-triazine. Master's thesis, School of Engineering and Science, 2011.

[7] M. K. Amosa, I. A. Mohammed, and S. A. Yaro. Sulphide scavengers in oil and gas industry - a review. *NAFTA*, pages 85–92, 2010.

[8] United States Department of Labor. Hydrogen sulfide - hazards. Online, feb 2016. https://www.osha.gov/SLTC/hydrogensulfide/hazards.html.

[9] Josefine Rønn Jakobsen. Synthesis and characterisation of algae-derived porous carbons. Technical report, Aalborg University Esbjerg, 2016.

[10] Susse Wegeberg and Claus Felby. Introduktion til alger. Online, apr 2010. http://bio4bio.ku.dk/documents/nyheder/wegeberg-intro-til-alger.pdf.

[11] Ernest Callenbach. *Ecology : A Pocket Guide*. University of California Press, 2008.

[12] Ditte Nan Hansen. Blære tang. Online, feb 2016. http://www.fugleognatur.dk/artsbeskrivelse.asp?ArtsID=4356.

[13] J. R. Miranda, P. C. Passarinho, and L. Gouveia. Pre-treatment optimization of scenedesmus obliquus microalga for bioethanol production. *Bioresource Technology*, 104:342–348, 2012.

[14] Encyclopedia Britannica. Green algae, feb 2016. http://academic.eb.com.

[15] Mike Morgan. Images of desmids from the genus scenedesmus. Online, feb 2016. http://www.microscopy-uk.org.uk/mag/indexmag.html?http://www.microscopy-uk.org.uk/mag/artoct05/mmdesmid.html.

[16] Dr. Robbe Wunschiers. The organism. Online, feb 2016. http://www.uni-koeln.de/ aei53/PhotoHydrogen/biore_02.htm.

[17] N. Ferrera-Lorenzo, E. Fuente, I. Suarez-Ruiz, and B. Ruiz. Koh activated carbon from conventional and microwave heating system of a macroalgae waste from the agar-agar industry. *Fluid Processing Technology*, 121:25–31, 2014.

[18] R. Aravindhan, J. Raghava Rao, and B. Unni Nair. Preparation and characterization of activated carbon from marine macro-algal biomass. *Journal of Hazardous Materials*, 162:688–694, 2009.

[19] Marie-Julie Pintor, Corine Jean-Marius, Valerie Jeanne-Rose, Pierre-Louis Taberna, Patrice Simon, Jean Gamby, Roger Gadiou, and Sarra Gaspard. Preparation of activated carbon from turbinaria turbinata seaweeds and its use as supercapacitor electrode materials. *Comptes Redus Chimie*, 16:73–79, 2013.

[20] Aravindhan Rathinam, Jonnalagadda Raghava Rao, and Balachandran Unni Nair. Adsorption of phenol onto activated carbon from seaweed: Determination of the optimal experimental parameters using factorial design. *Journal of the Taiwan Institute of Chemical Engineers*, 42:952–956, 2011.

[21] M.A. Lillo-Rodenas, J. Juan-Juan, D. Cazorla-Amoros, and A. Linares-Solano. About reactions occurring during chemical activation with hydroxides. *Carbon*, 42:1371–1375, 2004.

[22] A. Ahmadpour and D. D. Do. The preparation of active carbons from coal by chemical and physical activation. *Carbon*, 34(4):471–479, 1996.

[23] T.C. Drage, A. Arenillas, K.M. Smith, C. Pevida, S Piippo, and C. E. Snape. Preparation of carbon dioxide adsorbents from the chemical activation of urea-formaldehyde and melamine-formaldehyde resins. *Fuel*, 86:22–31, 2007.

[24] Ferhan Cecen and Ozgur Aktas. *Activated Carbon for Water and Wastewater Treatment*. John Wiley and Sons, 2011.

[25] Duncan W. Bruce, Dermot O'Hare, and Richard I. Walton. *Inorganic Materials Series : Multi Length-Scale Characterisation : Inorganic Materials Series*. John Wiley & Sons, 2013.

[26] Jean Rouquerol, Francoise Rouquerol, and S. W. Kenneth. *Adsorption by Powders and Porous Solids*. Academic Press, 1998.

[27] Scadinavian Culture Collection of Algae and Protozoa. Mwc/mwc+se. Online, feb 2016. http://www.sccap.dk/media/freshwater/3.asp.

[28] Ru-Ling Tseng and Szu-Kung Tseng. Pore structure and adsorption performance of the koh-activated carbons prepared from corncob. *Journal of Colloid and Interface Science*, pages 428–437, 2005.

[29] Fenghua Bai, Yongde Xia, Binling Chen, Haiquan Su, and Yanqiu Zhu. Preparation and carbon dioxide uptake capacity of n-doped porous carbon materials derived from direct carbonization of zeolitic imidazolate framework. *Carbon*, 79:213–226, 2014.

[30] Markus Klose, Katja Pinkert, Martin Zier, Martin Uhlemann, Florian Wolke, Tony Jaumann, Philipp Jehnichen, Daniel Wadewitz, Steffen Oswald, Ju rgen Eckert, and Lars Giebeler. Hollow carbon nano-onions with hierarchical porosity derived from commercial metal organic framework. *Carbon*, 79:302–309, 2014.

[31] Volker Presser, John McDonough, Sun-Hwa Yeon, and Yury Gogotsi. Effect on pore size on carbon dioxide sorption by carbide derived carbon. *Energy & envirenmental science*, 4:3059–3066, 2011.

[32] A. Esmaeili, S. Ghasemi, and J. Sohrabipour. Biosorption of copper from wastewater by activated carbon preparation from alga sargassum sp. *Natural Product Research*, 24(4):341–348, 2010.

[33] Akbar Esmaeili, Samira Ghasemi, and Abdolhossein Rustaiyan. Evaluation of the activated carbon prepared from the algae gracilaria for the biosorption of cu(ii) from aqueous solutions. *African Journal of Biotechnology*, 7(12):2034–2037, 2008.

[34] A. Esmaeili, P. Beirami, and S. Ghasemi. Evaluation of the marine algae gracilaria and its activated carbon for the adsorption of ni(ii) from wastewater. *E-Journal of Chemistry*, 8(4):1512–1521, 2011.

[35] L. R. Van Loon and M. A. Glaus. Review of the kinetics of alkaline degradation of cellulose in view of its relevance for safety assesment of radioactive waste repositories. *Journal of Environmental Polymer Degradation*, 5(2):97–109, 1997.

[36] Paul C Heimenz and Raj Rajagopalan. *Principles of Colloid and Surface Chemistry*. Marcel Dekker, third edition, 1997.

[37] A.K. Ladavos, A.P. Katsoulidis, A. Iosifidis, K.S. Triantafyllidis, T.J. Pinnavaia, and P.J. Pomonis. The bet equation, the inflection points of n2 adsorption isotherms and the estimation of specific surface area of porous solids. *Microporous and Mesoporous Materials*, 151:126–133, 2012.

[38] E. I. Shkol'nikov and E. V. Sidorova. Analytical equation for calculating the pore size distribution from adsorption data. *Doklady Physical Chemistry*, 412:4–7, 2007.

[39] D. Dolllimore and G. R. Heal. An improved method for the calculation of pore size distribution from adsorption data. *Journal of Applied Chemistry*, 1964.

[40] PerkinElmer, Inc., 940 Winter Street Waltham, MA 02451 USA. *2400 Series II CHNS/O Elemental Analysis*.

[41] www.ucl.ac.uk. Chn elemental microanalysis. Online, apr 2016.

[42] Richard Cammack, Teresa Atwood, Peter Campbell, Howard Parish, Anthony Smith, Frank Vella, and John Stirling. Oxford dictionary of biochemistry and molecular biology. Online, apr 2016. http://www.oxfordreference.com/view/10.1093/acref/9780198529170.001.0001/acref-9780198529170-e-7432?rskey=LG73tO&result=7342.

[43] Thermal conductivity of some common materials and gases. Online, may 2016. http://www.engineeringtoolbox.com/thermal-conductivity-d_429.html.

[44] Barbara H. Stuart. *Analytical Techniques in the Sciences (AnTs) * : Infrared Spectroscopy : Fundamentals and Applications (1)*. Wiley, 2004.

[45] Is carbon dioxide ir inactive? Online, may 2016. http://chemistry.stackexchange.com/questions/19119/is-carbon-dioxide-ir-inactive.